University of Alberta

Numerical Characterization of Ultrasound Elastography for the Early Detection of Deep Tissue Injuries

by

Kenton Hamaluik

A thesis submitted to the Faculty of Graduate Studies and Research in partial fulfilment of the requirements for the degree of

Master of Science

Department of Mechanical Engineering

Fall 2013
Edmonton, Alberta

Abstract

Deep tissue injuries are subcutaneous regions of extreme tissue breakdown generally induced by the application of significant mechanical pressure over extended periods of time through the biological mechanisms of ischemia and cell deformation causing rupture. These wounds are commonly suffered as a secondary wound or disease, often formed due to extended periods of motionless such as stationary sitting in spinal cord injured patients or those undergoing surgery.

Acknowledgements

Lorem ipsum dolor sit amet, consectetuer adipiscing elit. Ut purus elit, vestibulum ut, placerat ac, adipiscing vitae, felis. Curabitur dictum gravida mauris. Nam arcu libero, nonummy eget, consectetuer id, vulputate a, magna. Donec vehicula augue eu neque. Pellentesque habitant morbi tristique senectus et netus et malesuada fames ac turpis egestas. Mauris ut leo. Cras viverra metus rhoncus sem. Nulla et lectus vestibulum urna fringilla ultrices. Phasellus eu tellus sit amet tortor gravida placerat. Integer sapien est, iaculis in, pretium quis, viverra ac, nunc. Praesent eget sem vel leo ultrices bibendum. Aenean faucibus. Morbi dolor nulla, malesuada eu, pulvinar at, mollis ac, nulla. Curabitur auctor semper nulla. Donec varius orci eget risus. Duis nibh mi, congue eu, accumsan eleifend, sagittis quis, diam. Duis eget orci sit amet orci dignissim rutrum.

Contents

List of Tables

List of Figures

Chapter 1

Introduction

Chapter 2

Literature Review

2.1 Introduction

2.2 Deep Tissue Injuries

- Hospital-acquired presssure ulcers: a comparison of costs in medical vs. surgical patients [1]
- Pressure ulcer research funding in America: creation and analysis of an on-line database [2]
- Pressure ulcers in America: prevalence, incidence, and implications for the future. An executive summary of the National Pressure Ulcer Advisory Panel monograph [3]
- Hospitalzations related to pressure ulcers among adults 18 years and older, 2006: statistical brief no. 64 [4]
- Pressure ulcers in the elderly: analysis of prevalence and risk factors [5]
- Assessment and management of pressure ulcers in the elderly: current strategies [6]

- Pressure ulcers: the great insult [7]
- Reducing pressure ulcer prevalence rates in the long-term acute care setting [8]
- In-hopsital medical complications, length of stay, and mortality among stroke unit patients [9]
- Tracking quality over time: what do pressure ulcer data show? [10]

2.2.1 Aetiology and Histology

- Compression induced damage and internal tissue strains are related [11]
- Microstructural analusis of deformation-induced hypoxic damage in skeletal muscle [12]
- How does muscle stiffness affect the internal deformatins within the soft tissue layers of the buttocks under constant loading? [13]
- A theoretical model to study the effects of cellular stiffening on the damage eveolution in deep tissue injury [14]
- The biomechanics of sitting-acquired pressure ulcers in patients with spinal cord injury or lesions [15]
- Assessment of mechanical conditions in sub-dermal tissues during sitting: a combined expeirmental-MRI and finite-element approach [16]
- Mechanical gluteal soft tissue material parameter validation under complex tissue loading [17]
- Diffusion of water in skeletal muscle tissue is not influenced by compression in a rat model of deep tissue injury [18].

- Pressure ulcer risk factors among hospitalized patients with activity limitation [19]
- The etiology of pressure ulcers: skin deep or muscle bound? [20]
- Recurrence of initial pressure ulcer in persons with spinal cord injuries [21]
- Histopathology of pressure ulcers as a result of sequential computer-controller pressure sessions in a fuzzy rat model [22]
- National Pressure Ulcer Advisory Panel's Updated Pressure Ulcer Staging System [23]
- Diffusion of ulcers in the diabetic foot is promoted by stiffening of plantar muscular tissue under excessive bone compression [24]
- Risk factors for a pressure-related deep tissue injury: a theoretical mode [25]
- Deep tissue injury: how deep is our understanding? [26]
- Deep tissue injury from a bioengineering point of view [27]
- Distribution of internal pressure around bony prominences: implications to deep tissue injury and effectiveness of intermittent electrical stimulation [28]
- Distribution of internal strains around bony prominences in pigs [29]
- The importance of internal strain as opposed to interface pressure in the prevention of pressure related deep tissue injury [30]
- Stress analyses coupled with damage laws to determine biomechanical risk factors for deep tissue injury during sitting [31]

- Decubitus ulcers: role of pressure and friction in causation [32]
- Etiologic factors in pressure sores: an experimental model [33]
- In vivo muscle stiffening under bone compression promotes deep pressure sore [34]
- Pressure ulcers: avoidable or unavoidable? Results of the National Pressure Ulcer Advisory Panel Consensus Conference [35]
- The decubitus ulcer: facts and controversies [36]
- Mechanical compression-indeced pressure sores in rat hindlimb: muscle stiffness, histology, and computational models [37]

2.2.2 Detection

- Combination of thermographic and ultrasonographic assessments for early detection of deep tissue injury [38]
- A review of deep tissue injury development, detection, and prevention [39]
- Pressure ulcer knowledge in medical residents: an opportunity for improvement [40]
- Clinical nurse' knowledge and visual differentiation ability in pressure ulcer classification system and incontinence-associated dermatitis [41]
- Toward real-time detection of deep tissue injury risk in wheelchair users using Hertz contact theory [42]
- Compression-induced deep tissue injury examined with magnetic resonance imaging and histology [43]

- Low-echoic lesions underneath the skin in subjects with spinal-cord injury [44]
- National Pressure Ulcer Advisory Panel's Updated Pressure Ulcer Staging System [23]
- A new pressure ulcer risk assessment scale for individuals with spinal cord injury [45]
- Deep tissue engineering from a bioengineering point of view [27]
- Evaluation of four non-invasive methods for examination and characterization of pressure ulcers [46]
- Which techniques to improve the early detection and prevention of pressure ulcers? [47]
- Inception and validation of a pressure ulcer risk scale in oncology [48]
- Assessment and management of pressure ulcers in the elderly: current strategies [6]
- Reliability testing of the national database of nursing quality indicators pressure ulcer indicator [49]
- Ultrasound assessment of deep tissue injury in pressure ulcers: possible prediction of pressure ulcer progression [50]
- 3D ultrasound elastography for early detection of lesions. Evaluation on a pressure ulcer mimicking phantom [51]

2.2.3 Prevention and Treatment

- Prevention of deep tissue injury through muscle contractions induced by intermittent electrical stimulation after spinal cord injury in pigs [52]

- The importance of internal strain as opposed to interface pressure in the prevention of pressure related deep tissue injury [30]

- New methodology for preventing pressure ulcers using actimetry and autonomous nervous system recording [53]

- Pressure ulcers: the great insult [7]

- Reaching for the moon: achieving zero pressure ulcer prevalence, an update [54]

- Distribution of Internal Pressure around Bony Prominences: Implications to deep tissue injury and effectiveness of intermittent electrical stimulation [28]

- Distribution of internal strains around bony prominences in pigs **solid12-03**

- Reaching for the moon: achieving zero pressure ulcer prevalence, an update. [54]

- Reducing pressure ulcers in hip fracture patients [55]

- Reducing pressure ulcer prevalence rates in the long-term acute care setting [8]

- Development of pressure ulcer program across a university health system [56]

- Assessment and management of pressure ulcers in the elderly: current strategies [6]

- Pressure ulcers: the great insult [7]

- Intermittent electrical stimulation redistributes pressure and promotes tissue oxygenation in loaded muscles of individuals with spinal cord injury. [57]

2.3 Ultrasound Elastography

Lorem ipsum dolor sit amet, consectetuer adipiscing elit. Ut purus elit, vestibulum ut, placerat ac, adipiscing vitae, felis. Curabitur dictum gravida mauris. Nam arcu libero, nonummy eget, consectetuer id, vulputate a, magna. Donec vehicula augue eu neque. Pellentesque habitant morbi tristique senectus et netus et malesuada fames ac turpis egestas. Mauris ut leo. Cras viverra metus rhoncus sem. Nulla et lectus vestibulum urna fringilla ultrices. Phasellus eu tellus sit amet tortor gravida placerat. Integer sapien est, iaculis in, pretium quis, viverra ac, nunc. Praesent eget sem vel leo ultrices bibendum. Aenean faucibus. Morbi dolor nulla, malesuada eu, pulvinar at, mollis ac, nulla. Curabitur auctor semper nulla. Donec varius orci eget risus. Duis nibh mi, congue eu, accumsan eleifend, sagittis quis, diam. Duis eget orci sit amet orci dignissim rutrum.

2.3.1 Quasi-Static Ultrasound Elastography

- A new method for the visualization and quantification of internal skin elasticity by ultrasound imaging [58]

2.3.2 Acoustic Radiation Force Impulse Imaging

- derp

2.3.3 Shear Wave Speed Quantification

- derp

2.4 Numerical Characterization / Finite-Element Modelling

Lorem ipsum dolor sit amet, consectetuer adipiscing elit. Ut purus elit, vestibulum ut, placerat ac, adipiscing vitae, felis. Curabitur dictum gravida mauris. Nam arcu libero, nonummy eget, consectetuer id, vulputate a, magna. Donec vehicula augue eu neque. Pellentesque habitant morbi tristique senectus et netus et malesuada fames ac turpis egestas. Mauris ut leo. Cras viverra metus rhoncus sem. Nulla et lectus vestibulum urna fringilla ultrices. Phasellus eu tellus sit amet tortor gravida placerat. Integer sapien est, iaculis in, pretium quis, viverra ac, nunc. Praesent eget sem vel leo ultrices bibendum. Aenean faucibus. Morbi dolor nulla, malesuada eu, pulvinar at, mollis ac, nulla. Curabitur auctor semper nulla. Donec varius orci eget risus. Duis nibh mi, congue eu, accumsan eleifend, sagittis quis, diam. Duis eget orci sit amet orci dignissim rutrum.

2.5 Conclusion

Lorem ipsum dolor sit amet, consectetuer adipiscing elit. Ut purus elit, vestibulum ut, placerat ac, adipiscing vitae, felis. Curabitur dictum gravida mauris. Nam arcu libero, nonummy eget, consectetuer id, vulputate a, magna. Donec vehicula augue eu neque. Pellentesque habitant morbi tristique senectus et netus et malesuada fames ac turpis egestas. Mauris ut leo. Cras viverra metus rhoncus sem. Nulla et lectus vestibulum urna fringilla ultrices. Phasellus eu

tellus sit amet tortor gravida placerat. Integer sapien est, iaculis in, pretium quis, viverra ac, nunc. Praesent eget sem vel leo ultrices bibendum. Aenean faucibus. Morbi dolor nulla, malesuada eu, pulvinar at, mollis ac, nulla. Curabitur auctor semper nulla. Donec varius orci eget risus. Duis nibh mi, congue eu, accumsan eleifend, sagittis quis, diam. Duis eget orci sit amet orci dignissim rutrum.

References

[1] K. Beckrich and S. A. Aronovitch, "Hospital-acquired pressure ulcers: a comparison of costs in medical vs. surgical patients.," *Nursing economic$*, vol. 17, no. 5, pp. 263–271, 1999, ISSN: 0746-1739. [Online]. Available: http://view.ncbi.nlm.nih.gov/pubmed/10711175.

[2] J. M. Zanca, D. M. Brienza, D. Berlowitz, R. G. Bennett, C. H. Lyder, and National Pressure Ulcer Advisory Panel, "Pressure ulcer research funding in America: creation and analysis of an on-line database.," *Advances in skin & wound care*, vol. 16, no. 4, pp. 190–197, 2003, ISSN: 1527-7941. [Online]. Available: http://view.ncbi.nlm.nih.gov/pubmed/12897675.

[3] "Pressure ulcers in America: prevalence, incidence, and implications for the future. An executive summary of the National Pressure Ulcer Advisory Panel monograph.," *Advances in skin & wound care*, vol. 14, no. 4, pp. 208–215, 2001, ISSN: 1527-7941. [Online]. Available: http://view.ncbi.nlm.nih.gov/pubmed/11902346.

[4] C. Russo, C. Steiner, and W. Spector, "Hospitalizations Related to Pressure Ulcers Among Adults 18 Years and Older, 2006: Statistical Brief No. 64.," *Agency for Health Care Policy and Research (US)*, Dec. 2008. [Online]. Available: http://www.ncbi.nlm.nih.gov/sites/entrez?Db=pubmed%5C&%5C#38;Cmd=ShowDetailView%5C&%5C#38;TermToSearch=21595131.

[5] M. C. C. de Freitas, A. B. F. B. Medeiros, M. V. C. V. Guedes, P. C. C. de Almeida, F. T. T. de Galiza, and J. d. M. d. e. . M. Nogueira, "[Pressure ulcers in the elderly: analysis of prevalence and risk factors].," *Revista gaúcha de enfermagem / EENFUFRGS*, vol. 32, no. 1, pp. 143–150,

Mar. 2011, ISSN: 0102-6933. [Online]. Available: http://view.ncbi.nlm.nih.gov/pubmed/21888215.

[6] E. Jaul, "Assessment and management of pressure ulcers in the elderly: current strategies.," *Drugs & aging*, vol. 27, no. 4, pp. 311–325, Apr. 1, 2010, ISSN: 1170-229X. DOI: 10.2165/11318340-000000000-00000. [Online]. Available: http://dx.doi.org/10.2165/11318340-000000000-00000.

[7] J. Maklebust, "Pressure ulcers: the great insult.," *The Nursing clinics of North America*, vol. 40, no. 2, pp. 365–389, Jun. 2005, ISSN: 0029-6465. DOI: 10.1016/j.cnur.2004.09.015. [Online]. Available: http://dx.doi.org/10.1016/j.cnur.2004.09.015.

[8] C. T. Milne, D. Trigilia, T. L. Houle, S. Delong, and D. Rosenblum, "Reducing pressure ulcer prevalence rates in the long-term acute care setting.," *Ostomy/wound management*, vol. 55, no. 4, pp. 50–59, Apr. 2009, ISSN: 0889-5899. [Online]. Available: http://view.ncbi.nlm.nih.gov/pubmed/19387096.

[9] A. Ingeman, G. Andersen, H. H. Hundborg, M. L. Svendsen, and S. P. Johnsen, "In-hospital medical complications, length of stay, and mortality among stroke unit patients.," *Stroke; a journal of cerebral circulation*, vol. 42, no. 11, pp. 3214–3218, Nov. 2011, ISSN: 1524-4628. DOI: 10.1161/strokeaha.110.610881. [Online]. Available: http://dx.doi.org/10.1161/strokeaha.110.610881.

[10] L. Gunningberg and N. A. Stotts, "Tracking quality over time: what do pressure ulcer data show?" *International journal for quality in health care : journal of the International Society for Quality in Health Care / ISQua*, vol. 20, no. 4, pp. 246–253, Aug. 2008, ISSN: 1353-4505. DOI:

10.1093/intqhc/mzn009. [Online]. Available: http://dx.doi.org/10.1093/intqhc/mzn009.

[11] K. K. Ceelen, A. Stekelenburg, S. Loerakker, G. J. Strijkers, D. L. Bader, K. Nicolay, F. P. Baaijens, and C. W. Oomens, "Compression-induced damage and internal tissue strains are related.," *Journal of biomechanics*, vol. 41, no. 16, pp. 3399–3404, Dec. 5, 2008, ISSN: 0021-9290. DOI: 10.1016/j.jbiomech.2008.09.016. [Online]. Available: http://dx.doi.org/10.1016/j.jbiomech.2008.09.016.

[12] K. K. Ceelen, C. W. Oomens, and F. P. Baaijens, "Microstructural analysis of deformation-induced hypoxic damage in skeletal muscle.," *Biomechanics and modeling in mechanobiology*, vol. 7, no. 4, pp. 277–284, Aug. 2008, ISSN: 1617-7959. DOI: 10.1007/s10237-007-0097-7. [Online]. Available: http://dx.doi.org/10.1007/s10237-007-0097-7.

[13] S. Loerakker, L. R. Solis, D. L. Bader, F. P. Baaijens, V. K. Mushahwar, and C. W. Oomens, "How does muscle stiffness affect the internal deformations within the soft tissue layers of the buttocks under constant loading?" *Computer methods in biomechanics and biomedical engineering*, vol. 16, no. 5, pp. 520–529, 2013, ISSN: 1476-8259. DOI: 10.1080/10255842.2011.627682. [Online]. Available: http://dx.doi.org/10.1080/10255842.2011.627682.

[14] T. Nagel, S. Loerakker, and C. W. Oomens, "A theoretical model to study the effects of cellular stiffening on the damage evolution in deep tissue injury.," *Computer methods in biomechanics and biomedical engineering*, vol. 12, no. 5, pp. 585–597, Oct. 2009, ISSN: 1476-8259. DOI: 10.1080/10255840902788603. [Online]. Available: http://dx.doi.org/10.1080/10255840902788603.

[15] A. Gefen, "The biomechanics of sitting-acquired pressure ulcers in patients with spinal cord injury or lesions.," *International wound journal*, vol. 4, no. 3, pp. 222–231, Sep. 2007, ISSN: 1742-4801. DOI: 10.1111/j.1742-481x.2007.00330.x. [Online]. Available: http://dx.doi.org/10.1111/j.1742-481x.2007.00330.x.

[16] E. Linder-Ganz, N. Shabshin, Y. Itzchak, and A. Gefen, "Assessment of mechanical conditions in sub-dermal tissues during sitting: a combined experimental-MRI and finite element approach.," *Journal of biomechanics*, vol. 40, no. 7, pp. 1443–1454, 2007, ISSN: 0021-9290. DOI: 10.1016/j.jbiomech.2006.06.020. [Online]. Available: http://dx.doi.org/10.1016/j.jbiomech.2006.06.020.

[17] C. Then, J. Menger, T. J. Vogl, F. Hübner, and G. Silber, "Mechanical gluteal soft tissue material parameter validation under complex tissue loading.," *Technology and health care*, vol. 17, no. 5-6, pp. 393–401, 2009, ISSN: 1878-7401. DOI: 10.3233/thc-2009-0560. [Online]. Available: http://dx.doi.org/10.3233/thc-2009-0560.

[18] B. J. van Nierop, A. Stekelenburg, S. Loerakker, C. W. Oomens, D. Bader, G. J. Strijkers, and K. Nicolay, "Diffusion of water in skeletal muscle tissue is not influenced by compression in a rat model of deep tissue injury.," *Journal of biomechanics*, vol. 43, no. 3, pp. 570–575, Feb. 10, 2010, ISSN: 1873-2380. DOI: 10.1016/j.jbiomech.2009.07.043. [Online]. Available: http://dx.doi.org/10.1016/j.jbiomech.2009.07.043.

[19] R. M. Allman, P. S. Goode, M. M. Patrick, N. Burst, and A. A. Bartolucci, "Pressure ulcer risk factors among hospitalized patients with activity limitation.," *JAMA : the journal of the American Medical As-*

sociation, vol. 273, no. 11, pp. 865–870, Mar. 15, 1995, ISSN: 0098-7484. [Online]. Available: http://view.ncbi.nlm.nih.gov/pubmed/7869557.

[20] C. V. Bouten, C. W. Oomens, F. P. Baaijens, and D. L. Bader, "The etiology of pressure ulcers: skin deep or muscle bound?" *Archives of physical medicine and rehabilitation*, vol. 84, no. 4, pp. 616–619, Apr. 2003, ISSN: 0003-9993. DOI: 10.1053/apmr.2003.50038. [Online]. Available: http://dx.doi.org/10.1053/apmr.2003.50038.

[21] Z. B. Niazi, C. A. Salzberg, D. W. Byrne, and M. Viehbeck, "Recurrence of initial pressure ulcer in persons with spinal cord injuries.," *Advances in wound care : the journal for prevention and healing*, vol. 10, no. 3, pp. 38–42, 1997, ISSN: 1076-2191. [Online]. Available: http://view.ncbi.nlm.nih.gov/pubmed/9306777.

[22] R. Salcido, J. C. Donofrio, S. B. Fisher, E. K. LeGrand, K. Dickey, J. M. Carney, R. Schosser, and R. Liang, "Histopathology of pressure ulcers as a result of sequential computer-controlled pressure sessions in a fuzzy rat model.," *Advances in wound care : the journal for prevention and healing*, vol. 7, no. 5, Sep. 1994, ISSN: 1076-2191. [Online]. Available: http://view.ncbi.nlm.nih.gov/pubmed/7889250.

[23] J. Black, M. Baharestani, J. Cuddigan, B. Dorner, L. Edsberg, D. Langemo, M. E. E. Posthauer, C. Ratliff, G. Taler, and National Pressure Ulcer Advisory Panel, "National Pressure Ulcer Advisory Panel's updated pressure ulcer staging system.," *Dermatology nursing / Dermatology Nurses' Association*, vol. 19, no. 4, Aug. 2007, ISSN: 1060-3441. [Online]. Available: http://view.ncbi.nlm.nih.gov/pubmed/17874603.

[24] A. Gefen and E. Linder-Ganz, "[Diffusion of ulcers in the diabetic foot is promoted by stiffening of plantar muscular tissue under excessive bone

compression].," *Der Orthopäde*, vol. 33, no. 9, pp. 999–1012, Sep. 2004, ISSN: 0085-4530. DOI: 10.1007/s00132-004-0701-9. [Online]. Available: http://dx.doi.org/10.1007/s00132-004-0701-9.

[25] A. Gefen and E. Haberman, "Viscoelastic properties of ovine adipose tissue covering the gluteus muscles.," *Journal of biomechanical engineering*, vol. 129, no. 6, pp. 924–930, Dec. 2007, ISSN: 0148-0731. DOI: 10.1115/1.2800830. [Online]. Available: http://dx.doi.org/10.1115/1.2800830.

[26] A. Stekelenburg, D. Gawlitta, D. L. Bader, and C. W. Oomens, "Deep tissue injury: how deep is our understanding?" *Archives of physical medicine and rehabilitation*, vol. 89, no. 7, pp. 1410–1413, Jul. 2008, ISSN: 1532-821X. DOI: 10.1016/j.apmr.2008.01.012. [Online]. Available: http://dx.doi.org/10.1016/j.apmr.2008.01.012.

[27] A. Gefen, "Deep tissue injury from a bioengineering point of view.," *Ostomy/wound management*, vol. 55, no. 4, pp. 26–36, Apr. 2009, ISSN: 0889-5899. [Online]. Available: http://view.ncbi.nlm.nih.gov/pubmed/19387094.

[28] L. R. Solis, A. Liggins, R. R. Uwiera, N. Poppe, E. Pehowich, P. Seres, R. B. Thompson, and V. K. Mushahwar, "Distribution of Internal Pressure around Bony Prominences: Implications to Deep Tissue Injury and Effectiveness of Intermittent Electrical Stimulation.," *Annals of biomedical engineering*, pp. 1–20, Feb. 22, 2012, ISSN: 1521-6047. DOI: 10.1007/s10439-012-0529-0. [Online]. Available: http://dx.doi.org/10.1007/s10439-012-0529-0.

[29] L. R. Solis, A. B. Liggins, P. Seres, R. R. Uwiera, N. R. Poppe, E. Pehowich, R. B. Thompson, and V. K. Mushahwar, "Distribution of Internal Strains Around Bony Prominences in Pigs.," *Annals of biomedical*

engineering, pp. 1–19, Mar. 8, 2012, ISSN: 1521-6047. DOI: 10.1007/s10439-012-0539-y. [Online]. Available: http://dx.doi.org/10.1007/s10439-012-0539-y.

[30] C. W. Oomens, S. Loerakker, and D. L. Bader, "The importance of internal strain as opposed to interface pressure in the prevention of pressure related deep tissue injury.," *Journal of tissue viability*, vol. 19, no. 2, pp. 35–42, May 2010, ISSN: 0965-206X. DOI: 10.1016/j.jtv.2009.11.002. [Online]. Available: http://dx.doi.org/10.1016/j.jtv.2009.11.002.

[31] E. Linder-Ganz and A. Gefen, "Stress analyses coupled with damage laws to determine biomechanical risk factors for deep tissue injury during sitting.," *Journal of biomechanical engineering*, vol. 131, no. 1, Jan. 2009, ISSN: 0148-0731. DOI: 10.1115/1.3005195. [Online]. Available: http://dx.doi.org/10.1115/1.3005195.

[32] S. M. Dinsdale, "Decubitus ulcers: role of pressure and friction in causation.," *Archives of physical medicine and rehabilitation*, vol. 55, no. 4, pp. 147–152, Apr. 1974, ISSN: 0003-9993. [Online]. Available: http://view.ncbi.nlm.nih.gov/pubmed/4595834.

[33] R. K. Daniel, D. L. Priest, and D. C. Wheatley, "Etiologic factors in pressure sores: an experimental model.," *Archives of physical medicine and rehabilitation*, vol. 62, no. 10, pp. 492–498, Oct. 1981, ISSN: 0003-9993. [Online]. Available: http://view.ncbi.nlm.nih.gov/pubmed/7305643.

[34] A. Gefen, N. Gefen, E. Linder-Ganz, and S. S. Margulies, "In vivo muscle stiffening under bone compression promotes deep pressure sores.," *Journal of biomechanical engineering*, vol. 127, no. 3, pp. 512–524, Jun.

2005, ISSN: 0148-0731. [Online]. Available: http://view.ncbi.nlm.nih.gov/pubmed/16060358.

[35] J. M. Black, L. E. Edsberg, M. M. Baharestani, D. Langemo, M. Goldberg, L. McNichol, J. Cuddigan, and National Pressure Ulcer Advisory Panel, "Pressure ulcers: avoidable or unavoidable? Results of the National Pressure Ulcer Advisory Panel Consensus Conference.," *Ostomy/-wound management*, vol. 57, no. 2, pp. 24–37, Feb. 2011, ISSN: 1943-2720. [Online]. Available: http://view.ncbi.nlm.nih.gov/pubmed/21350270.

[36] C. Campbell and L. C. C. Parish, "The decubitus ulcer: facts and controversies.," *Clinics in dermatology*, vol. 28, no. 5, pp. 527–532, Sep. 2010, ISSN: 1879-1131. DOI: 10.1016/j.clindermatol.2010.03.010. [Online]. Available: http://dx.doi.org/10.1016/j.clindermatol.2010.03.010.

[37] E. Linder-Ganz and A. Gefen, "Mechanical compression-induced pressure sores in rat hindlimb: muscle stiffness, histology, and computational models.," *Journal of applied physiology (Bethesda, Md. : 1985)*, vol. 96, no. 6, pp. 2034–2049, Jun. 2004, ISSN: 8750-7587. DOI: 10.1152/japplphysiol.00888.2003. [Online]. Available: http://dx.doi.org/10.1152/japplphysiol.00888.2003.

[38] T. Higashino, G. Nakagami, T. Kadono, Y. Ogawa, S. Iizaka, H. Koyanagi, S. Sasaki, N. Haga, and H. Sanada, "Combination of thermographic and ultrasonographic assessments for early detection of deep tissue injury.," *International wound journal*, Nov. 22, 2012, ISSN: 1742-481X. DOI: 10.1111/j.1742-481x.2012.01117.x. [Online]. Available: http://dx.doi.org/10.1111/j.1742-481x.2012.01117.x.

[39] A. Gefen, K. J. Farid, and I. Shaywitz, "A review of deep tissue injury development, detection, and prevention: shear savvy.," *Ostomy/wound management*, vol. 59, no. 2, pp. 26–35, Feb. 2013, ISSN: 1943-2720. [Online]. Available: http://view.ncbi.nlm.nih.gov/pubmed/23388395.

[40] J. M. Levine, E. A. Ayello, K. M. Zulkowski, and J. Fogel, "Pressure ulcer knowledge in medical residents: an opportunity for improvement.," *Advances in skin & wound care*, vol. 25, no. 3, pp. 115–117, Mar. 2012, ISSN: 1538-8654. DOI: 10.1097/01.asw.0000412908.43335.46. [Online]. Available: http://dx.doi.org/10.1097/01.asw.0000412908.43335.46.

[41] Y. J. J. Lee, S. Park, J. Y. Y. Kim, C. G. G. Kim, and S. K. K. Cha, "[Clinical nurses' knowledge and visual differentiation ability in pressure ulcer classification system and incontinence-associated dermatitis].," *Journal of Korean Academy of Nursing*, vol. 43, no. 4, pp. 526–535, Aug. 2013, ISSN: 2093-758X. DOI: 10.4040/jkan.2013.43.4.526. [Online]. Available: http://dx.doi.org/10.4040/jkan.2013.43.4.526.

[42] L. Agam and A. Gefen, "Toward real-time detection of deep tissue injury risk in wheelchair users using Hertz contact theory.," *Journal of rehabilitation research and development*, vol. 45, no. 4, 2008, ISSN: 1938-1352. [Online]. Available: http://view.ncbi.nlm.nih.gov/pubmed/18712639.

[43] A. Stekelenburg, C. W. Oomens, G. J. Strijkers, K. Nicolay, and D. L. Bader, "Compression-induced deep tissue injury examined with magnetic resonance imaging and histology.," *Journal of applied physiology (Bethesda, Md. : 1985)*, vol. 100, no. 6, pp. 1946–1954, Jun. 2006, ISSN:

8750-7587. DOI: 10.1152/japplphysiol.00889.2005. [Online]. Available: http://dx.doi.org/10.1152/japplphysiol.00889.2005.

[44] N. Kanno, T. Nakamura, M. Yamanaka, K. Kouda, T. Nakamura, and F. Tajima, "Low-echoic lesions underneath the skin in subjects with spinal-cord injury.," *Spinal cord*, vol. 47, no. 3, pp. 225–229, Mar. 2009, ISSN: 1362-4393. DOI: 10.1038/sc.2008.101. [Online]. Available: http://dx.doi.org/10.1038/sc.2008.101.

[45] C. A. Salzberg, D. W. Byrne, C. G. Cayten, P. van Niewerburgh, J. G. Murphy, and M. Viehbeck, "A new pressure ulcer risk assessment scale for individuals with spinal cord injury.," *American journal of physical medicine & rehabilitation / Association of Academic Physiatrists*, vol. 75, no. 2, pp. 96–104, 1996, ISSN: 0894-9115. [Online]. Available: http://view.ncbi.nlm.nih.gov/pubmed/8630201.

[46] E. Sloth and T. Karlsmark, "Evaluation of four non-invasive methods for examination and characterization of pressure ulcers.," *Skin research and technology : official journal of International Society for Bioengineering and the Skin (ISBS) [and] International Society for Digital Imaging of Skin (ISDIS) [and] International Society for Skin Imaging (ISSI)*, vol. 14, no. 3, pp. 270–276, Aug. 2008, ISSN: 1600-0846. DOI: 10.1111/j.1600-0846.2008.00290.x. [Online]. Available: http://dx.doi.org/10.1111/j.1600-0846.2008.00290.x.

[47] C. Gehin, E. Brusseau, R. Meffre, P. M. Schmitt, J. F. Deprez, and A. Dittmar, "Which techniques to improve the early detection and prevention of pressure ulcers?" *Conference proceedings : ... Annual International Conference of the IEEE Engineering in Medicine and Biology Society. IEEE Engineering in Medicine and Biology Society. Conference*,

vol. 1, pp. 6057–6060, 2006, ISSN: 1557-170X. DOI: 10.1109/iembs.2006.259506. [Online]. Available: http://dx.doi.org/10.1109/iembs.2006.259506.

[48] I. Fromantin, M. C. Falcou, A. Baffie, C. Petot, R. Mazerat, C. Jaouen, L. Téot, and d. Rycke, "Inception and validation of a pressure ulcer risk scale in oncology.," *Journal of wound care*, vol. 20, no. 7, Jul. 2011, ISSN: 0969-0700. [Online]. Available: http://view.ncbi.nlm.nih.gov/pubmed/21841721.

[49] S. Hart, S. Bergquist, B. Gajewski, and N. Dunton, "Reliability testing of the National Database of Nursing Quality Indicators pressure ulcer indicator.," *The Journal of nursing administration*, vol. 40, no. 10 Suppl, Oct. 2010, ISSN: 1539-0721. DOI: 10.1097/nna.0b013e3181f37d15. [Online]. Available: http://dx.doi.org/10.1097/nna.0b013e3181f37d15.

[50] N. Aoi, K. Yoshimura, T. Kadono, G. Nakagami, S. Iizuka, T. Higashino, J. Araki, I. Koshima, and H. Sanada, "Ultrasound assessment of deep tissue injury in pressure ulcers: possible prediction of pressure ulcer progression.," *Plastic and reconstructive surgery*, vol. 124, no. 2, pp. 540–550, Aug. 2009, ISSN: 1529-4242. DOI: 10.1097/prs.0b013e3181addb33. [Online]. Available: http://dx.doi.org/10.1097/prs.0b013e3181addb33.

[51] J.-F. F. Deprez, G. Cloutier, C. Schmitt, C. Gehin, A. Dittmar, O. Basset, and E. Brusseau, "3D ultrasound elastography for early detection of lesions. evaluation on a pressure ulcer mimicking phantom.," *Conference proceedings : ... Annual International Conference of the IEEE Engineering in Medicine and Biology Society. IEEE Engineering in Medicine and Biology Society. Conference*, vol. 2007, pp. 79–82, 2007, ISSN: 1557-

170X. DOI: 10.1109/iembs.2007.4352227. [Online]. Available: http://dx.doi.org/10.1109/iembs.2007.4352227.

[52] L. R. Solis, E. Twist, P. Seres, R. B. Thompson, and V. K. Mushahwar, "Prevention of deep tissue injury through muscle contractions induced by intermittent electrical stimulation after spinal cord injury in pigs.," *Journal of applied physiology (Bethesda, Md. : 1985)*, vol. 114, no. 2, pp. 286–296, Jan. 15, 2013, ISSN: 1522-1601. DOI: 10.1152/japplphysiol.00257.2012. [Online]. Available: http://dx.doi.org/10.1152/japplphysiol.00257.2012.

[53] R. Meffre, C. Gehin, P. M. Schmitt, F. De Oliveira, and A. Dittmar, "New methodology for preventing pressure ulcers using actimetry and autonomous nervous system recording.," *Conference proceedings : ... Annual International Conference of the IEEE Engineering in Medicine and Biology Society. IEEE Engineering in Medicine and Biology Society. Conference*, vol. 1, pp. 5563–5566, 2006, ISSN: 1557-170X. DOI: 10.1109/iembs.2006.259352. [Online]. Available: http://dx.doi.org/10.1109/iembs.2006.259352.

[54] I. Bales and T. Duvendack, "Reaching for the moon: achieving zero pressure ulcer prevalence, an update.," *Journal of wound care*, vol. 20, no. 8, Aug. 2011, ISSN: 0969-0700. [Online]. Available: http://view.ncbi.nlm.nih.gov/pubmed/21841712.

[55] M. Thompson, "Reducing pressure ulcers in hip fracture patients.," *British journal of nursing (Mark Allen Publishing)*, vol. 20, no. 15, 2011, ISSN: 0966-0461. [Online]. Available: http://view.ncbi.nlm.nih.gov/pubmed/21841645.

[56] D. Carson, K. Emmons, W. Falone, and A. M. M. Preston, "Development of Pressure Ulcer Program Across a University Health System.," *Journal of nursing care quality*, Sep. 10, 2011, ISSN: 1550-5065. DOI: 10.1097/ncq.0b013e3182310f8b. [Online]. Available: http://dx.doi.org/10.1097/ncq.0b013e3182310f8b.

[57] S. Gyawali, L. Solis, S. L. L. Chong, C. Curtis, P. Seres, I. Kornelsen, R. Thompson, and V. K. Mushahwar, "Intermittent electrical stimulation redistributes pressure and promotes tissue oxygenation in loaded muscles of individuals with spinal cord injury.," *Journal of applied physiology (Bethesda, Md. : 1985)*, vol. 110, no. 1, pp. 246–255, Jan. 2011, ISSN: 1522-1601. DOI: 10.1152/japplphysiol.00661.2010. [Online]. Available: http://dx.doi.org/10.1152/japplphysiol.00661.2010.

[58] O. Osanai, M. Ohtsuka, M. Hotta, T. Kitaharai, and Y. Takema, "A new method for the visualization and quantification of internal skin elasticity by ultrasound imaging.," *Skin research and technology : official journal of International Society for Bioengineering and the Skin (ISBS) [and] International Society for Digital Imaging of Skin (ISDIS) [and] International Society for Skin Imaging (ISSI)*, Feb. 23, 2011, ISSN: 1600-0846. DOI: 10.1111/j.1600-0846.2010.00492.x. [Online]. Available: http://dx.doi.org/10.1111/j.1600-0846.2010.00492.x.

Chapter 3

Numerical Characterization of Quasi-Static Ultrasound Elastography

3.1 Introduction

The goal of this study was to numerically characterize various important parameters related to detecting DTI using quasi-static ultrasound elastography (such as lesion geometry, material properties, and transducer characteristics) in order to examine the feasibility of using the technique to detect early DTI in humans. Quasi-static ultrasound elastography involves displacing the surface of the skin such that internal tissues are placed under a strain field. Ultrasound signals are used to track internal strains which then relate to the localized mechanical stiffness of the tissue — local regions that are significantly more or less stiff than surrounding tissue may be classified as either undergoing rigor mortis or necrosis and may present cause for concern.

3.2 Method

In order to evaluate the sensitivity of using quasi-static ultrasound elastography to detect deep tissue injuries, a numerical model of these injuries was created such that a subset of the investigated cases mimicked a physical phantom model which was used for validation. This numerical model allowed the rapid modification of numerous parameters related to DTI to examine their effect on the method's detection sensitivity where detection sensitivity is defined as the slope of the given characterization plot. To fully understand the problem, 5 general model cases were studied with each case generating numerous sub-studies on the effect of various parameters relating to that case. These parameters included: lesion depth; lesion altitude (distance of the lesion above deep bone); lesion diameter; ratio of the stiffness between the lesion and the surrounding tissue; ultrasound probing frequency; strain level applied by the transducer; the separation distance between two co-located lesions; radius of a circular averaging filter applied to the lesion boundaries; the number of smaller clustered lesions per unit area; the radius of each individual clustered lesion; the width of the lesion in a Visible Human [1] model and the depth of the lesion in a Visible Human model. The range of values for the tested parameters are given in Table 3.1 which resulted in a total of 144 model cases that were analyzed. The geometry of the models shown in Fig. 3.1 include: a simple spherical lesion embedded within a 2-dimensional rectangular zone of soft tissue; two lesions located at the same depth separated laterally by a finite dimension, δ_{sep}; a spherical lesion without hard boundaries; a cluster of small lesions which together form a larger lesion area; and a lesion with mri-acquired geometry [2] embedded in geometry obtained from a Visible Human slice [1].

In Fig. 3.1e, the lesion is located superficial to the left ischial tuberosity in the transverse plane. The lesion geometry was obtained from an MRI scan

Table 3.1: Range of values of investigated parameters

Parameter	Symbol	Values
Lesion depth	d	$[3.5, 6.5, 8.5, 10.0]$ cm
Lesion altitude	h	$[1.25, 2.50, 3.75]$ cm
Lesion diameter	$\varnothing S$	$[0.5, 1.0, 2.0, 2.5]$ cm
Lesion stiffness ratio	E_{rel}	$[0.32, 0.56, 1.80, 3.20]$
Ultrasound frequency	f	$[2, 4, 8]$ MHz
Transudcer-applied strain	ε_{app}	$[2.5, 5.0, 10.0]$ %
Colocated separation distance	δ_{sep}	$[1.25, 1.50, 1.75, 2.00]$ cm
Blurred lesion blur radius	b_r	$[1.0, 2.5, 5.0, 7.5]$ mm
Clustered lesion density	b_ρ	$[10, 20, 30, 40]$ cm^{-2}
Clustered lesion radius	r_{bl}	$[0.5, 1.0, 1.5]$ mm
Visible human lesion width	$\varnothing S$	$[0.5, 1.0, 2.0, 2.5]$ cm
Visible human lesion depth	d	$[6.25, 6.75, 7.25]$ cm

of a real deep tissue injury induced in a porcine model [2]. The generic soft tissue in this model is modelled after muscle, with a layer of adipose tissue residing at the surface of the model.

Note that the axial direction referred to henceforth as the "axial" direction of an ultrasound transducer placed along the top (superficial) surface of the domain such that it becomes the "vertical" direction.

Simulated ultrasound images were acquired through the convolution of a point spread function with a normally distributed background map of scattering centres [3]. These images were then combined with a finite-element deformation model of the strained tissue to generate both pre- and post- compression images of the lesions and surrounding tissue. These images were fed into a tissue strain estimation algorithm to determine the detection sensitivity of the technique. Finally, the technique was validated against a physical phantom model using a subset of the simulated cases.

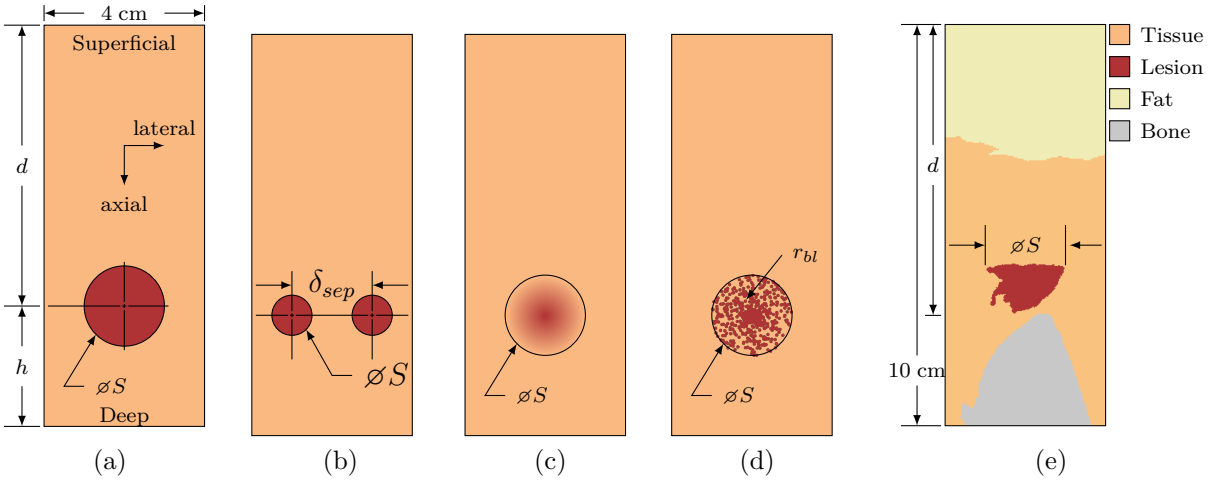

Figure 3.1: Model geometry showing the investigated lesions embedded in a 4 cm wide soft tissue domain. Axial and lateral directions mimic that of a typical ultrasound transducer placed along the top boundary of the domain. The simplest case of a circular lesion embedded in a soft tissue domain located superior to hard underlying bone is shown in (a). In order to investigate the interference caused by closely-located lesions, the case shown in (b) was investigated. Because of the relatively unknown and variable geometric properties of deep tissue injury lesions, cases (c) and (d) were investigated where the lesion edges were blurred and the lesion was actually a large collection of small lesions, respectively. Finally, to investigate detection sensitivity in a realistic setting, case (e) was investigated where an mri-acquired deep tissue injury was overlaid on a slice from the Visible Human Project such that the injury lesion was located immediately superior to an ischial tuberosity.

3.2.1 Formation of B-Mode Ultrasound Images

Through the convolution of a point spread function and a normal random distribution of scattering centres, simulated ultrasound images were generated. The point spread function was defined axially as a cosine function operating at the ultrasound probing frequency modulated by a Gaussian distribution defined by $\mu = 2\lambda$ and $\sigma = 2\lambda$ where λ is the wavelength of the ultrasonic probing waves. Laterally, the point spread function was modelled as a Gaussian distribution defined by $\mu = 0$ and $\sigma = 0.25w_{active}$ where w_{active} is the total width of the active transducer elements during scan-line acquisition. This resulted in the point spread function given in Fig. 3.2. Resulting images were

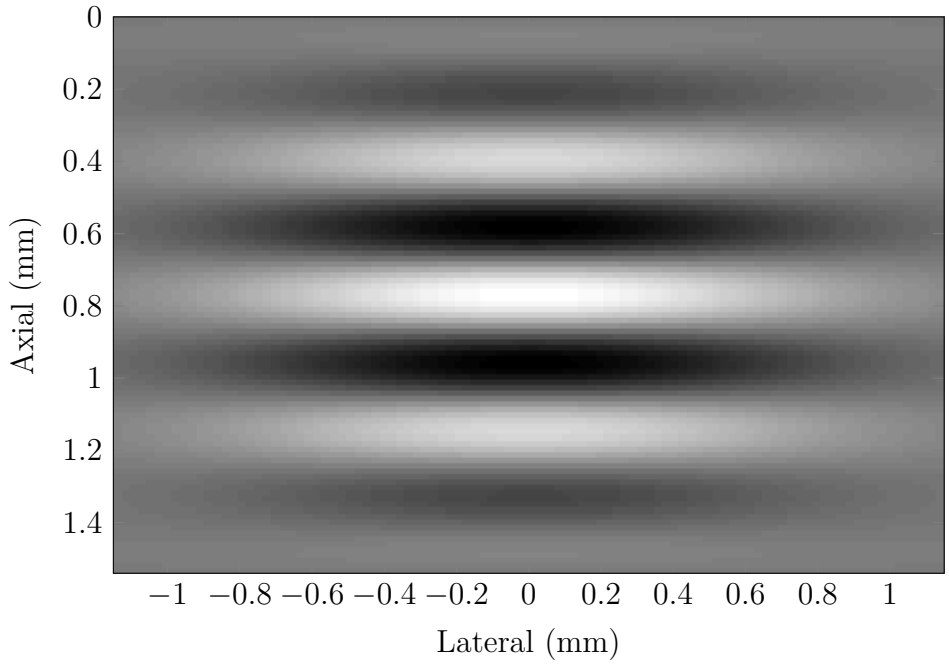

Figure 3.2: Point spread function used for simulating b-mode ultrasound scans. The function is defined axially by a cosine function at the probing frequency and modulated by a Gaussian function both axially and laterally.

composed of 192 scan lines each sampled at 50 MHz.

3.2.2 Finite-Element Model of Tissue Deformation Under Surface Distortion

As a response to an external load being applied to the boundary of a domain, internal structures deform. In the case of a relatively stiff deep tissue injury embedded within surrounding soft tissues, this implies that when the surface of the skin is depressed, the relatively stiff lesion will not strain to the same magnitude that the surrounding soft tissue does. In order to simulate the deformation of interrogated tissue, the displacement field for the simulated models was calculated according to:

$$-\nabla \cdot \sigma = F \tag{3.1}$$

Where σ is the Cauchy stress tensor and F are the applied body forces. Simulations were performed assuming a 2-dimensional linearly elastic material deformation model under plane strain conditions. A 3-dimensional model was also considered, however the deformations differed from the 2-dimensional simulation by less than 1 % so a 2-dimensional model was deemed adequate. Soft tissue was modelled using a Young's modulus of elasticity of 25 kPa, Poisson's ratio of 0.499, and density of 998 kg/m^3 [4]–[6]. The only difference in lesion mechanical properties from the surrounding soft tissue was the modulus of elasticity which varied according to the simulation parameters. The bottom of the domain was held fixed such that:

$$u = 0, \qquad \Gamma = \Gamma_{bottom} \tag{3.2}$$

While this boundary condition represents an idealized scenario, it may be likened to that of tissue located superficial to a relatively stiff anchoring bone below. This lower region is where deep tissue injuries generally form and is therefore of special importance. Compressive strains were applied to the top of the domain so as to induce strain along the top boundary:

$$u = (0, -u_0), \qquad \Gamma = \Gamma_{top} \tag{3.3}$$

From these simulations, displacement fields throughout the domain were calculated which were then used to displace tissue (including scattering centres) in the simulated ultrasound images in both the axial and lateral directions. This process resulted in pairs of pre- and post- compression simulated b-mode images of lesions of varying parameters which could then be analyzed and characterized.

3.2.3 Characterizing Quasi-Static Ultrasound Elastography

Utilizing a 2-D locally regularized tissue strain estimation algorithm [7], pairs of pre- and post- compression images were used to calculate elastogram estimations for the full range of parameter values of the simulated lesions. The algorithm consists of sweeping the image domain with a series of overlapping regions of interest (ROI). ROI are compared between pre- and post- compression images, with ROI in the post- compression images being axially scaled and translated and laterally translated versions of the same ROI in the pre-compression images.

Qualitatively, the noise and computation time of the resulting elastograms were found to be minimum when using an axial ROI size of approximately 10 times the ultrasound wavelength. Axial ROI overlap was held at 99 % to produce elastograms with minimal noise, even though this introduced significant increases in computation time. Due to the extreme anisotropic nature of ultrasound signals, lateral ROI size was kept to 5 signal widths with lateral ROI overlaps of 80 %.

3.2.4 Model Validation Using a Commercially Available Phantom

Utilizing a CIRS Elasticity QA Phantom model 049, a subset of the results obtained from the finite-element simulations and numerical characterizations were compared against their physical phantom equivalents. The phantom mimics acoustically homogeneous soft tissue with embedded lesions which vary in depth, size, and mechanical stiffness. Mechanical properties of the phantom as given by manufacturer specifications are summarized in Table 3.2. Pre- and

Table 3.2: CIRS Phantom Model Mechanical Properties

Property	Value
Nominal basal stiffness	25 kPa
Lesion stiffness	$[8, 14, 45, 80]$ kPa
Speed of sound	1540 m/s
Acoustic attenuation	0.5 dB/cm MHz
Lesion diameter	$[10, 20]$ mm
Lesion depth	$[15, 35]$ mm

post- compression b-mode ultrasound images were obtained of each lesion in the phantom and the resulting strain ratio for that lesion was compared to the simulated strain ratio for that combination of parameters. Specifically, lesions at a depth of 3.5 cm, a diameter of 2.0 cm, and with true stiffness ratios of 0.56, 1.80, and 3.20 were examined. Surface indentation was performed manually with the transducer indenting approximately 0.5 cm (6.25 %) at the surface.

3.3 Results

Following the procedure outlined in Section 3.2, finite-element models of ultrasonic b-mode image formation and tissue deformation were synthesized. The results of these models were then fed into the local strain estimation algorithm described in Section 3.2.3. The resulting numerical characterizations of the relationship between measured and true strain ratios in the simulated tissue and their dependence on the various lesion parameters given in Table 3.1 were examined. Finally, the local strain estimation algorithm was carried out on a physical phantom and compared against a subset of the simulated cases.

3.3.1 Finite Element Models of Ultrasound and Deformation

Sample images generated using both the acoustic and deformation finite-element models are given in Figs. 3.3a, 3.3b and 3.3c. In Fig. 3.3a, a sample generated b-mode ultrasound scan is given. Fig. 3.3b shows the vector-sum displacement field generated by the deformation finite-element model. The entire top surface of the model has been displaced axially by 6.25 mm (5 %), which caused deformation of both the soft tissue and embedded lesion within. Since the lesion was modelled as being 3.2 times stiffer than the surrounding tissue, the lesion underwent less strain which consequently resulted in the lesser displacement depicted. Fig. 3.3c shows the resultant b-mode image generated by applying the displacement field given in Fig. 3.3b to the tissue and embedded scattering centres used to create Fig. 3.3a. What results is a locally scaled and translated version of Fig. 3.3a that corresponds to indenting the surface of the skin above a stiff lesion. The large anechoic region located at the bottom of the domain is tissue that was not modelled in the pre-compression image as it was outside of the original domain. This area represents the region of tissue that is undetectable with the strain-estimation algorithm given in Section 3.2.3 as the information contained there is only available in one of the two input images and so is considered incomplete data.

3.3.2 Resulting Elastograms

The 2-D locally regularized tissue strain estimation algorithm described in Section 3.2.3 was used in combination with the simulated resultant b-mode ultrasound images (Figs. 3.3a and 3.3c) in order to generate elastogram images which were used in the subsequent analysis. An example elastogram resulting

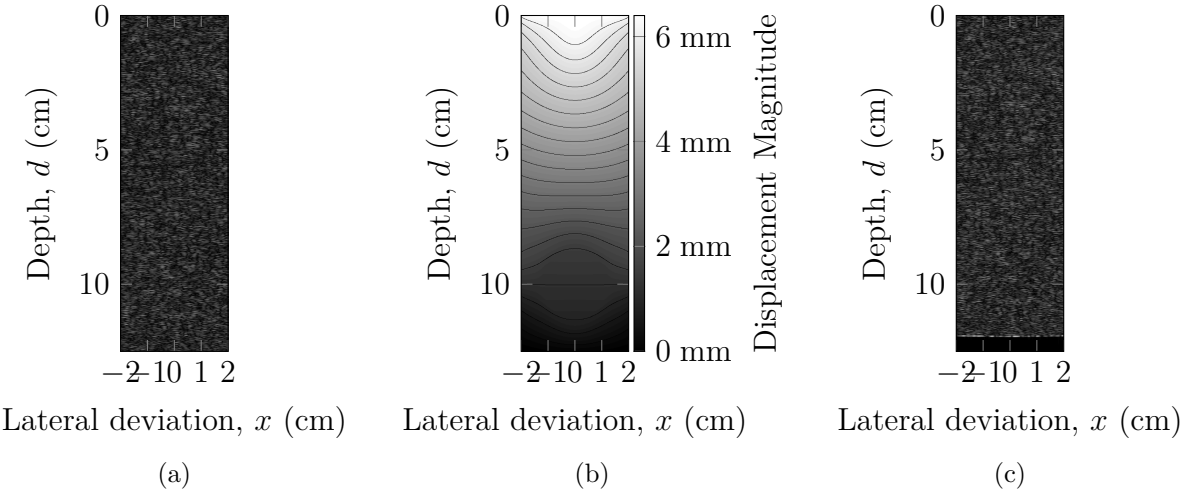

Figure 3.3: Finite-element model results for the case when $d = 10$ cm, $\varnothing S = 2.5$ cm, $\varepsilon_{rel} = 3.20$, and $f = 4$ MHz showing (a) a generated b-mode image of the pre-compressed tissue domain, (b) the vector-summed displacement field induced by compressive strain applied to the top of the boundary, and (c) a generated b-mode image of the post-compressed tissue domain. The included lesion is not visible in (a) and (c) as it's acoustic properties were no different than surrounding tissues. An anechoic region is visible along the bottom of the domain in (c) which represents tissue outside of the domain visible in (a).

from the simulation presented in Fig. 3.3 is shown in Fig. 3.4. Throughout the entire domain on this sample elastogram, regions outside of the stiff lesions showed compressive strains of approximately 5 % as expected due to the compression applied to the upper boundary of the model. The entire lesion region showed relatively consistent low strain amounts of approximately 2.5 %, which is consistent with the lesion being stiffer (and so straining less) than the surrounding tissue. Of note is the increased strain pattern which appeared both axially and laterally around the lesion. While generally symmetric about the axial direction, this stress field was largely concentrated above the lesion when the lesion was deep (close to the bone). This may be explained as a stress concentration brought about by the sudden change in mechanical material properties of the tissue and may serve to fuel the conditions of excessive cell deformation and ischemia which initiated the formation of a deep tissue

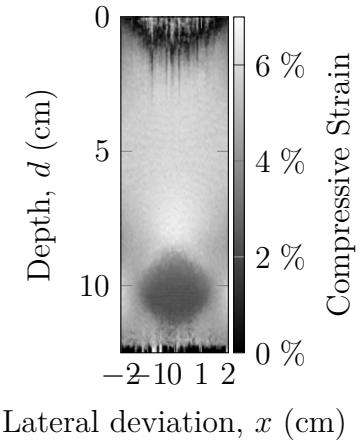

Figure 3.4: Sample strain elastogram showing estimated strain values for $d = 10$ cm, $\varnothing S = 2.5$ cm, $\varepsilon_{rel} = 3.20$, $f = 4$ MHz. While undetectable on a single b-mode image, the elastogram clearly shows a low-strain (stiff) lesion located approximately 10 cm from the surface.

injury in the first place, exacerbating the wound and assisting its expansion toward the surface.

3.3.3 Numerical Characterizations

In order to determine the sensitivity of using quasi-static ultrasound elastography to detect deep tissue injuries, elastograms such as the example that was calculated in Section 3.3.2 were calculated for the full range of parameters given in Table 3.1. "Measured" strain ratios for each elastogram were obtained by comparing the mean strain within each lesion with the mean engineering strain of the surrounding tissue such that:

$$\varepsilon_{rel,measured} = \frac{\varepsilon_{tissue}}{\varepsilon_{lesion}} \tag{3.4}$$

ε_{tissue} was sampled as the mean strain in the region of tissue with the same geometry as the lesion located immediately superficial to the lesion in all cases.

In order to characterize how each parameter of interest affects the detection

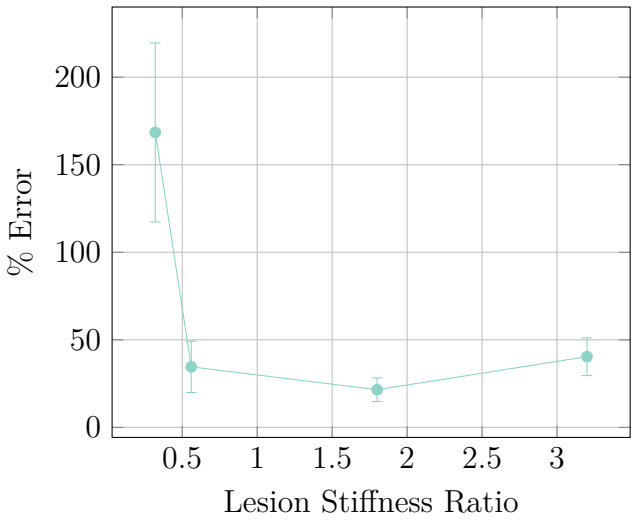

Figure 3.5: Detection ability as it related to true lesion stiffness ratio. For all but small lesion stiffness ratios (very soft "lesions"), results are linear and predictable. For small lesion stiffness ratios (0.32), the lesion becomes severely misrepresented. This is likely due to the algorithm "losing track" of scattering centers for the relatively large displacements induced in the signiciantly less stiff tissue.

sensitivity of quasi-static ultrasound elastography, measured strain ratios for various lesions were calculated and compared against $\varepsilon_{rel,true}$. $\varepsilon_{rel,true}$ is derived from the relative Young's modulus of elasticity of the lesion such that:

$$\varepsilon_{rel,true} = \frac{\varepsilon_{tissue}}{\varepsilon_{lesion}} = \frac{\left(\frac{\sigma_{applied}}{E_{tissue}}\right)}{\left(\frac{\sigma_{applied}}{E_{lesion}}\right)} = \frac{E_{lesion}}{E_{tissue}} \tag{3.5}$$

Fig. 3.5 portrays the severe error involved with using the methods described in Section 3.2 to investigate extremely low stiffness lesions. In nearly all investigated cases where the true lesion stiffness ratio was 0.32, the algorithms described severely misrepresented the measured strain ratio of the lesion, often portraying these extremely low stiffness regions as being more stiff than they truly were. It is hypothesized that the excessively large localized deformations in these lesions interrupted the algorithm's ability to sufficiently track the displacement of scattering centres within the tissue, lowering the

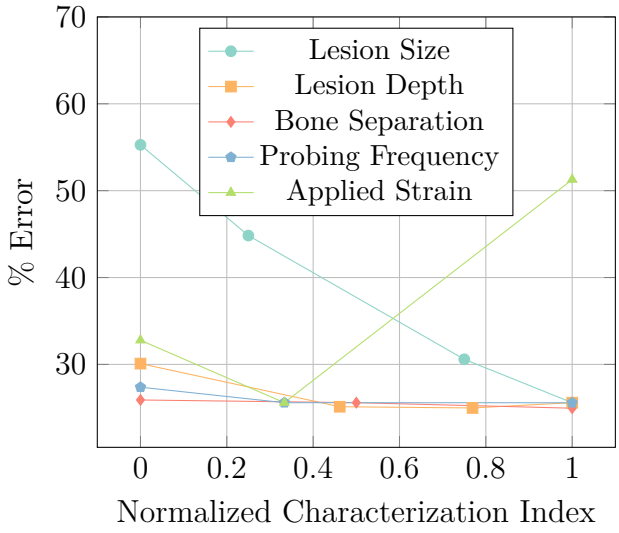

Figure 3.6: Error characterization for range of studied parameters for the simple model of a spherical lesion embedded within soft tissue as seen in Fig. 3.1a. Each parameter has been normalized to the range studied so overly-sensitive regions may be readily distinguished.

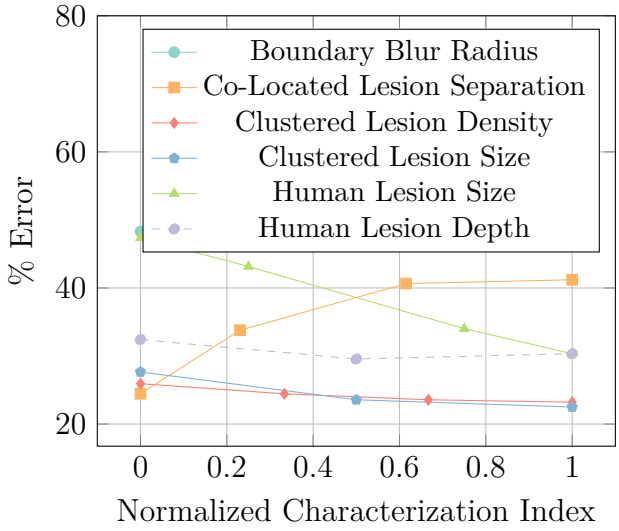

Figure 3.7: Error characterization for range of studied parameters for the co-located lesions, blurred boundary lesions, clustered lesions, and visible human lesion models as seen in Figs. 3.1b – 3.1e. Each parameter has been normalized to the range studied so overly-sensitive regions may be readily distinguished.

magnitude of displacement within the lesion and subsequently increasing it's "measured" strain ratio.

In order to broadly investigate the critical parameter-values of the inves-

tigated models, each parameter was normalized to it's investigated range and the error resulting over these ranges is given in Figs. 3.6 and 3.7.

In Fig. 3.6, it is clear to see that the most sensitive error-inducing situations occur when either the lesion is very small or if large strains are used to deform the tissue. Similarly, it is expected that if the lesion depth were increased much further, significant errors would arise with increasing depth. Logically, this may be explained due to the decreasing magnitude of displacement with increasing depth — at a certain point, the magnitude of displacement of scattering centres will be on par with the measurement noise, and the lesion will cease to be detectable.

From Fig. 3.7 it can be seen that small lesions in the Visible Human-MRI model as well as co-located lesions with large separation distances produce greater measurement errors. Conversely, lesion depth in the Visible Human-MRI model; lesion density and individual lesion size in the clustered lesion model; and boundary blur radius in the blurred-edges model do not seem to affect the measurement error significantly. Of note is the relative large amount of static error present in the boundary blur radius model which is hypothesized to be due to lesser mean tissue stiffness in the investigated region than expected.

Fig. 3.8 shows the relationship between lesion size and detection sensitivity for lesions at a depth of 10 cm in a model depth of 12.5 cm interrogated at 4 MHz with 5 % applied strain. Specifically, Fig. 3.8 shows the decreasing detection sensitivity with decreasing lesion size with the best detection sensitivity being with the largest investigated lesions with a diameter of 2.5 cm. On the opposite end, the detection sensitivity of lesions at or below 0.5 cm in diameter is questionable. This level of detection ability (with regards to lesion size) is acceptable, however, as although there is little data on the true size of

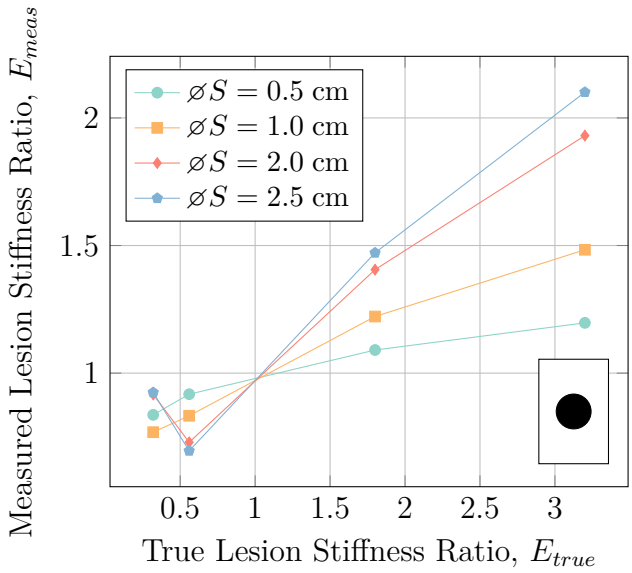

Figure 3.8: Lesion size characterization at a depth of 10 cm with a 4 MHz ultrasound probing frequency showing increasing detection sensitivity of the lesion with increasing lesion size. Detection sensitivity is less than ideal for all cases, with the best case being for lesions approximately 2.5 cm in diameter.

formative DTI, MRI results indicate that untreated deep tissue injuries are on the scale of multiple cm [2]. Thus, being able to detect lesions of at least 1 cm in diameter should prove to be adequate to both detect and monitor DTI.

In order to investigate the effect of lesion depth on the detection sensitivity, measured strain ratios for circular lesions with a diameter of 2.5 cm located at various depths were interrogated with a 4 MHz probing frequency, and strained by 5 %. The results of this investigation are seen in Fig. 3.9.

In Fig. 3.21, it can be seen there there was little interplay between detection sensitivity and measured strain ratios at the various depths examined for all but the case for very soft (mushy) lesions (with a stiffness ratio of 0.32). At such low stiffness ratios, the excessive tissue deformation interrupts the tissue strain estimation algorithm's ability to adequately track the induced displacements in the lesion.

Since the strain field caused by compressive forces near an extremely rigid

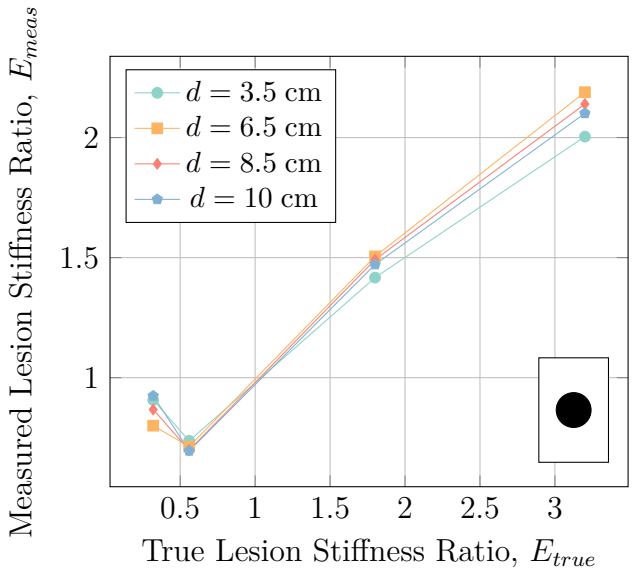

Figure 3.9: Lesion depth characterization at a lesion diameter of 2.5 cm with a 4 MHz ultrasound probing frequency generally showing general independence of detection sensitivity on lesion depth in the tissue.

structure embedded within a relatively soft domain will be significantly heterogeneous, the effect of lesion altitude above the underlying stiff bone was examined with the hypothesis that if the lesion were too close to the hard bone, it would be masked by the strain field caused by the bone's existence. A 2.5 cm diameter lesion was interrogated with a 4 MHz probing frequency and 5 % applied strain. The results of this characterization are given in Fig. 3.10.

In Fig. 3.10, it can be seen that the lesion altitude above the underlying bone had very little effect on the detection sensitivity. Although larger strain fields may be generated near the bone, it is hypothesized that the larger fields also extend larger and so affect healthy tissue to more or less the same degree as the forming lesion.

In order to characterize the effect of using alternate ultrasound probing frequencies, simulations were carried out on lesions using probing frequencies of 2 MHz, 4 MHz, and 8 MHz. The simulated lesions had a diameter of 2.5 cm, were located at a depth of 10 cm and we strain at 5 %. The results of this

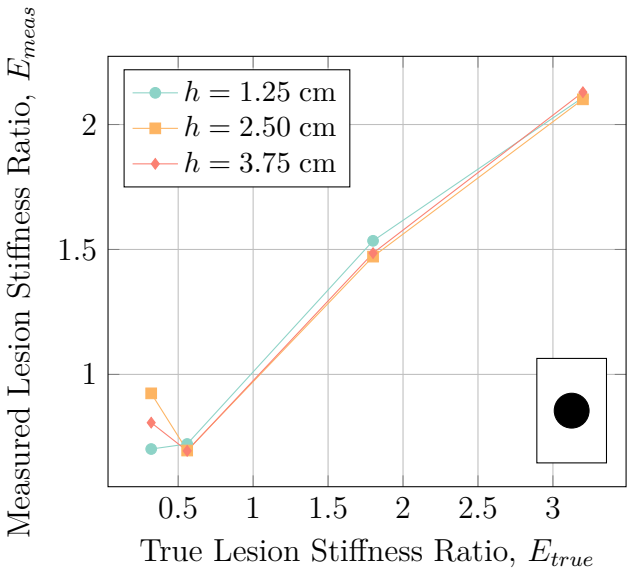

Figure 3.10: Effect of lesion altitude above the underlying bone. Aside from erroneous results at very low lesion stiffness ratios, the effect is negligible.

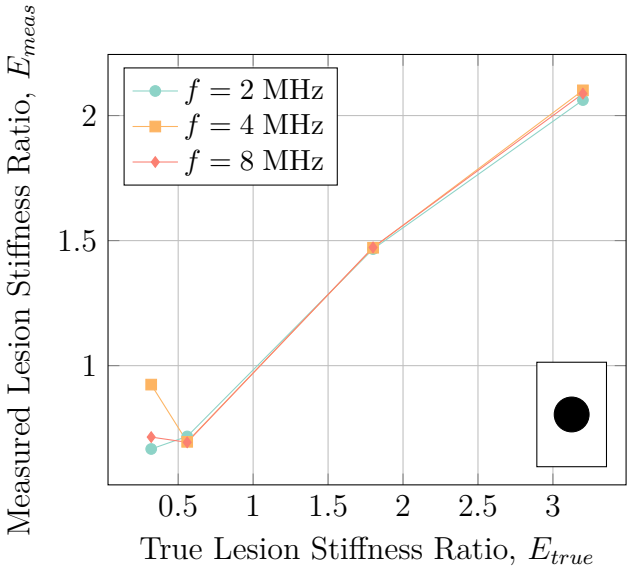

Figure 3.11: Characterization of ultrasonic probing frequency on detection sensitivity. Apart from the requirement of using an ultrasonic frequency low enough to interrogate the desired tissue, probing frequency has negligible effect on the detection sensitivity.

study are given in Fig. 3.11.

As can be seen from Fig. 3.11, there is very little effect on the detection sensitivity from the ultrasound probing frequency that was used, therefore an

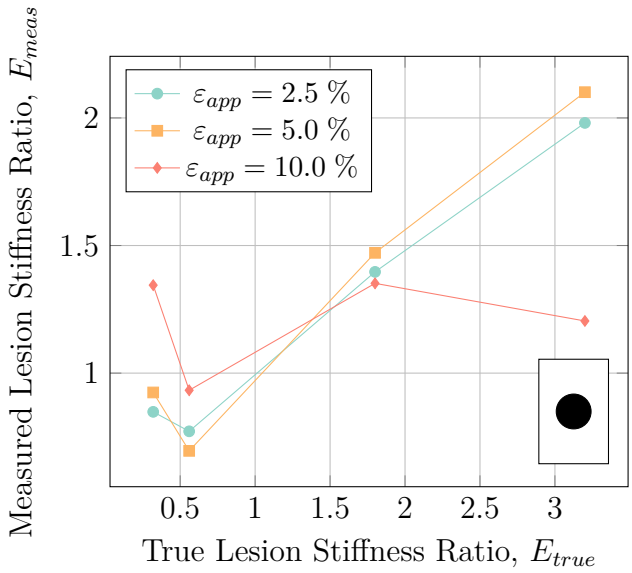

Figure 3.12: Applied strain characterization plot for lesions with a diamater of 2.5 cm located at a depth of 10 cm interrogated at 4 MHz. There is little difference between 2.5 % and 5.0 % applied strain, while large-magnitude strains of 10 % generate significant error for both very soft and very stiff lesions.

appropriate frequency should be chosen so as to reach the the full depth of the bone-muscle interface at suspected DTI locations while retaining the best image resolution.

As quasi-static ultrasound elastography is most likely to be performed via manual indentation where the exact magnitude of applied deformation is unknown, it is important to study the effect of applied strain magnitude on the detection sensitivity. Applied strains of 2.5 %, 5.0 %, and 10 % were investigated on a 2.5 cm diameter lesion at a depth of 10 cm using a probing frequency of 4 MHz; the results are given in Fig. 3.12.

While Fig. 3.12 shows a relatively constant detection sensitivity for compressive strains of 2.5 % and 5 %, compressive strains of 10 % generate significant measurement error for both very soft and very stiff lesions. Under large compressive strains, the tissue (either in the lesion as in the soft lesion case, or the surrounding tissue as in the stiff lesion case) deforms considerably which

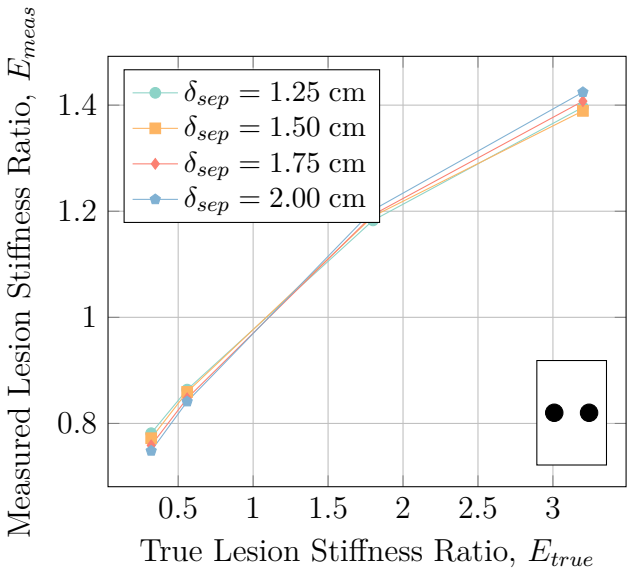

Figure 3.13: Effect of lesion separation distance on two 1.0 cm diameter lesions co-located at a depth of 10 cm interrogated with a 4 MHz probe with 5 % applied strain. There is no negligible difference between separation distances on the detection sensitivity.

again interferes with the algorithm's ability to properly track the displacement of tissue. It should also be noted that applying overly large strains to an already forming deep tissue injury may cause additional unwarranted damage. Thus it is imperative that applied surface indentation be kept to reasonable bounds ($2.5 - 5$ %, or $0.25 - 0.50$ cm in 10 cm deep domains), not only for safety of the tissue but also for clarity of the diagnostic test.

To study the effect that closely spaced lesions will have on the detection sensitivity as well as how discernible the lesions will be from each other, the separation distance between two 1.0 cm diameter co-located lesions at a depth of 10 cm was examined using a 4 MHz probing frequency with 5 % applied strain magnitude. The results of this study are shown in 3.13.

While Fig. 3.13 shows that the separation distance between co-located lesions causes a negligible effect on the detection sensitivity, Fig. 3.14 shows regions of decreased strain above and below the centreline of the lesions. While

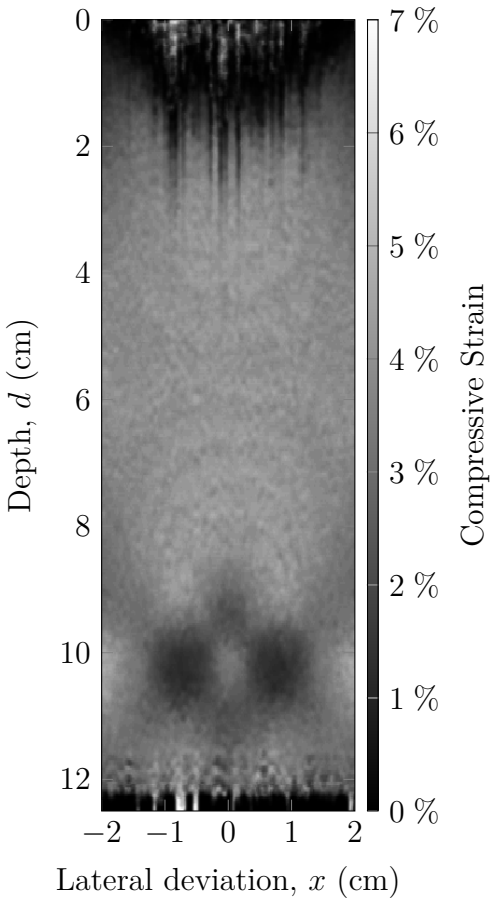

Figure 3.14: Elastogram for two co-located lesions of 1.0 cm diameter at a depth of 10 cm interrogated using a 4 MHz probing frequency with 5 % applied strain. A pattern of decreased strain is present above and below the centerline between the two lesions while the lesions themselves are not affected by each other.

these regions had the same basal stiffness as the bulk tissue, the decreased strain pattern may obfuscate the true results by introducing "phantom lesions" which are not actually present but merely the result of the existing lesions.

While the simulations performed thus far assumed that lesions were perfect spheres with hard boundaries in order to isolate specific parameters of interest, this assumption may not always be accurate. Rather, due to the nature of injury formation, lesions may form gradual boundaries that "fade" from stiff or necrotic tissue to healthy tissue. To investigate the effect of this phenomenon on the detection sensitivity, lesions with "blurred boundaries" were investi-

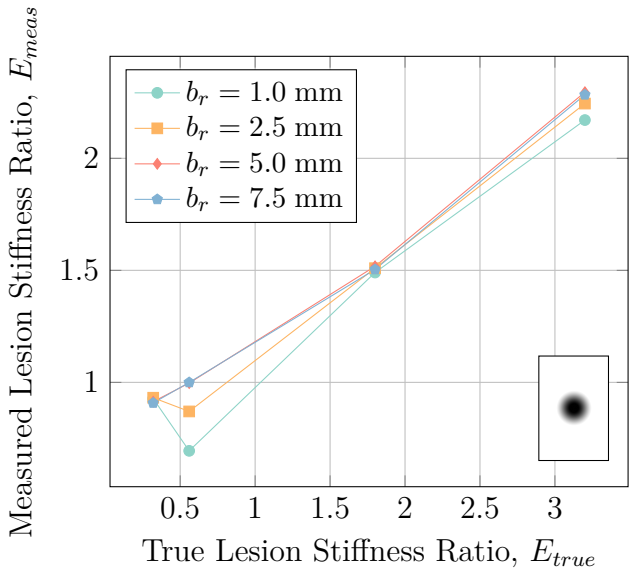

Figure 3.15: Characterization of the effect of lesion blur radius on lesion detection sensitivity for a 2.5 cm diameter lesion at a depth of 10 cm using a probing frequency of 4 MHz and applied strain of 5 %. While there is negligible effect of the blur radius on stiff lesions, the strain ratio for soft lesions is considerably over-estimated.

gated. Hard spherical lesions were blurred by convolving the lesion domain with a disc blurring kernel of varying radius. The results for this investigation on lesions with a diameter of 2.5 cm, at a depth of 10 cm and interrogated with a 4 MHz probing frequency with 5 % applied strain are given in Fig. 3.15.

Fig. 3.15 shows that there is very little dependence on the lesion detection sensitivity for stiff lesions (lesions with a stiffness ratio ≥ 1.0). However, for soft lesions, the tissue strain estimation algorithm seems to over-estimate the stiffness of the lesions.

Similar to how lesions may have "blurred boundaries" rather that hard ones, so too may lesion composition not be homogeneous. In order to study the effect of heterogeneous regions of injured tissue, the detection sensitivity of a set of numerous small lesions located within close proximity to each other so as to form a large, heterogeneous area of diseased tissue was examined. Fig. 3.16 shows the results for this model for varying numbers of 2 mm diameter

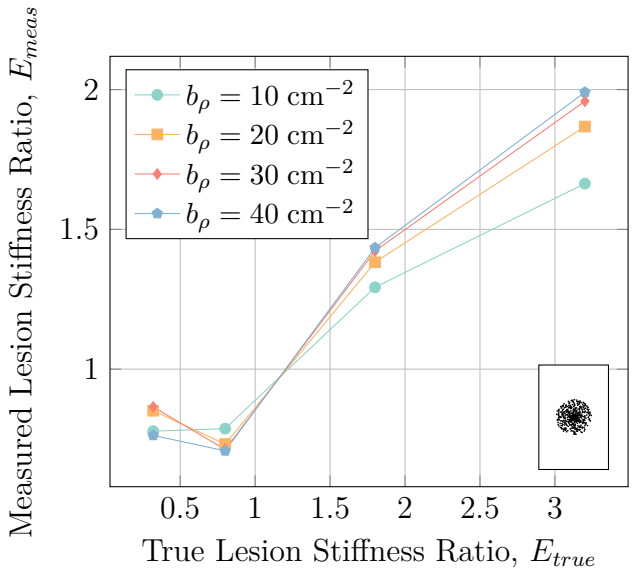

Figure 3.16: Characterization of lesion density for a group of numerous smaller 2 mm diameter lesions comprising a large area with a diameter of 2.5 cm at a depth of 10 cm interrogated with a 4 MHz probing frequency and 5 % applied strain. Detection sensitivity decreases with decreasing lesion density, as expected.

lesions in a 2.5 cm diameter circle located at a depth of 10 cm with a probing frequency of 4 MHz and 5 % applied strain. Fig. 3.18 further explores this model by investigating the case where there are 30 small lesions per square cm with individual lesions ranging in diameter from 0.5 mm to 1.5 mm.

The characterization plot in Fig. 3.16 for small lesion density is less linear than other characterization plots, with lesion density having a significant effect on the detection sensitivity. Specifically, for low lesion densities, the detection sensitivity is much lower than for high lesion densities. However, this observation is warranted after examination of the elastogram produced from these results, given in Fig. 3.17, which shows how the small lesions are not individually detected but rather the entire region is detected as one large lesion. Since the average stiffness ratio over this region is lesser than the stiffness ratio of individual lesions, it makes sense that the "measured" strain ratio will be less than expected.

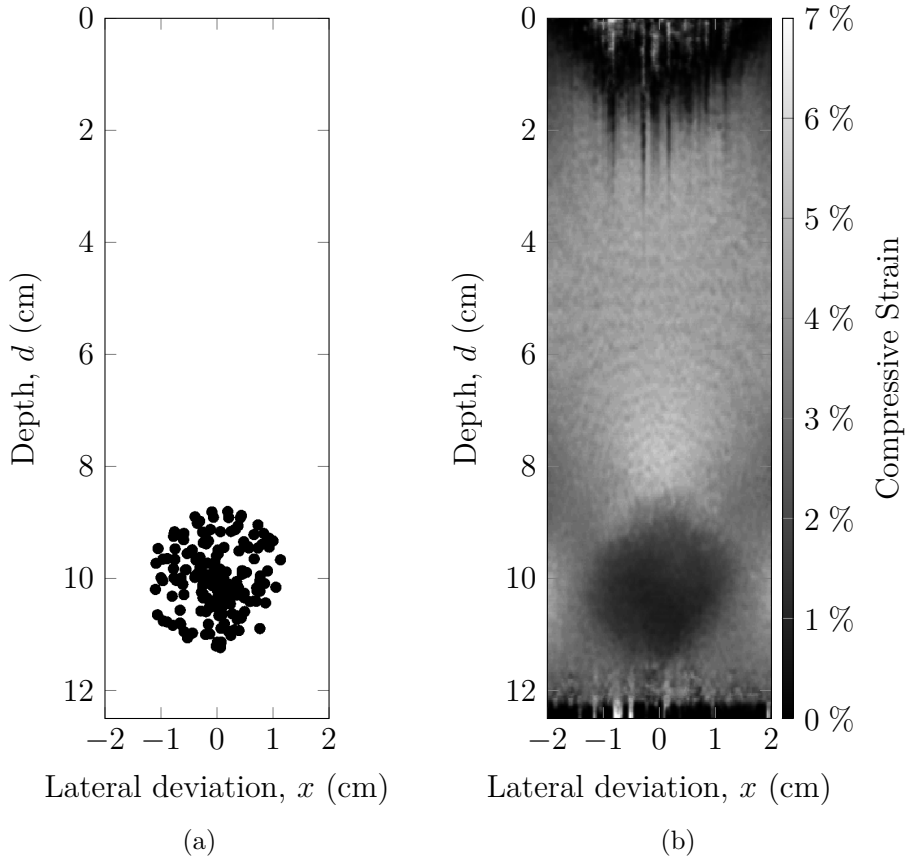

Figure 3.17: Stiffness map (a) and corresponding elastogram (b) for a group a small lesions with a density of 10 lesions per cm^2 grouped in a 2.5 cm diameter circle at a depth of 10 cm interrogated with a 4 MHz probing frequency and 5 % applied strain. In (a), white regions are regular tissue while black regions are the small lesions. In the elastogram, individual lesions do not stand out, rather the entire region of lesions appears as one large region of unhealthy tissue.

Similar to the results shown in Fig. 3.16, changing the size of the individual small lesions does have an effect on the measured strain. In this case, when individual lesions are small, the total area occupied by lesions is lesser which results in a lesser average tissue stiffness over the grouped lesion region.

Note that although the elastography algorithm was able to detect the larger lesion-filled regions in these simulations, it was completely unable to discern the individual lesions comprising those regions. This is not surprising due to both the generated strain fields in the healthy tissue throughout the larger

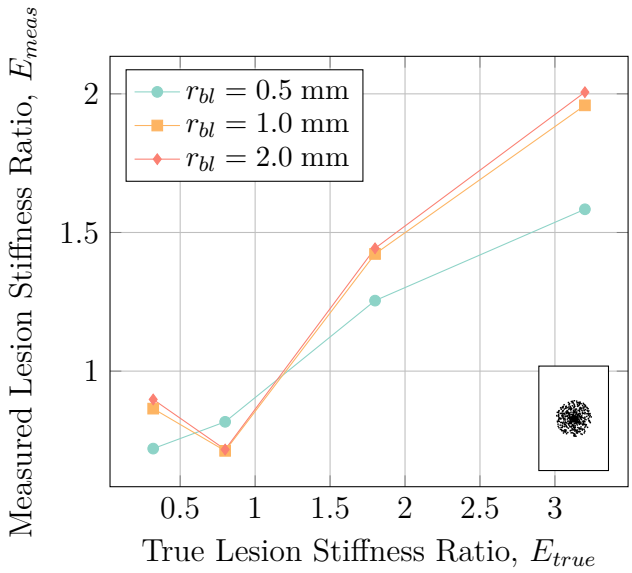

Figure 3.18: Characterization of lesion radius for a group of numerous smaller lesions with a density of 30 lesions per cm^2 comprising a large area with a diameter of 2.5 cm at a depth of 10 cm interrogated with a 4 MHz probing frequency and 5 % applied strain. Detection sensitivity decreases with decreasing individual lesion size, as expected.

lesion area as well as the results presented in Fig. 3.8 showing poor detection sensitivity for lesions with diameters $\leq$ 1 cm while the individual lesions in this simulation had diameters of the scale of 0.5 mm – 1.5 mm.

Finally, in order to place these results within the context of a likely real scenario in humans, a more complicated model utilizing an MRI-acquired lesion and slides from the Visible Human Project [1] was developed. Specifically, lesion geometry was taken from a real deep tissue injury in a pig model imaged using T_2^*-weighted MRI. The human geometry was taken from a transverse plane slice aross the left ischial tuberosity such that the lesion was placed immediately superficial to the boney promience. For this model, the overall lesion width and lesion depth were examined with results shown in Figs. 3.19 and 3.21 respectively.

In Fig. 3.19, it is clear to see than small lesions (with a diameter $\leq$ 1.0 cm) are almost impossible to adequately detect (although larger lesions will be

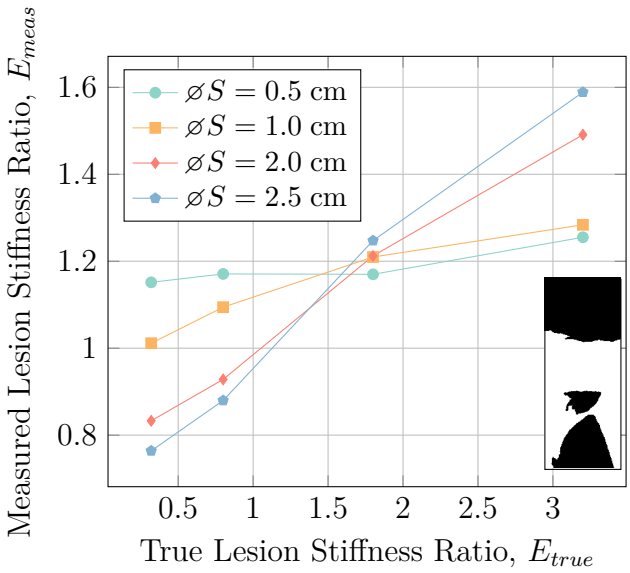

Figure 3.19: Characterization of lesion width in a Visible Human-MRI model for lesions at a depth of 7.25 cm interrogated with a 4 MHz probing frequency with 5 % applied strain. Small lesions (with a width $\leq$ 1.0 cm) are severely misrepresented and portray general over-estimation of lesion stiffness larger lesions.

adequately detectable). It is hypothesized that this phenomenon is due to the excessive strain apparent above the boney prominence that is seen in the resultant elastogram given in Fig. 3.20 such that the lesion is "washed out" by the strain field developed by the relatively stiff bone nearby.

In Fig. 3.21, there is little to no dependence of the detection sensitivity on the lesion depth in the Visible Human-MRI model with all depth curves displaying the same profile. However, deeper lesions (lesions closer to the bony prominence) have stiffnesses that are over-estimated with respect to their superficial counterparts. This is hypothesized to be due to the increased strain field present in all of the soft tissue located immediately superior to the bony prominence, but should not pose a serious problem for imaging lesions of this nature.

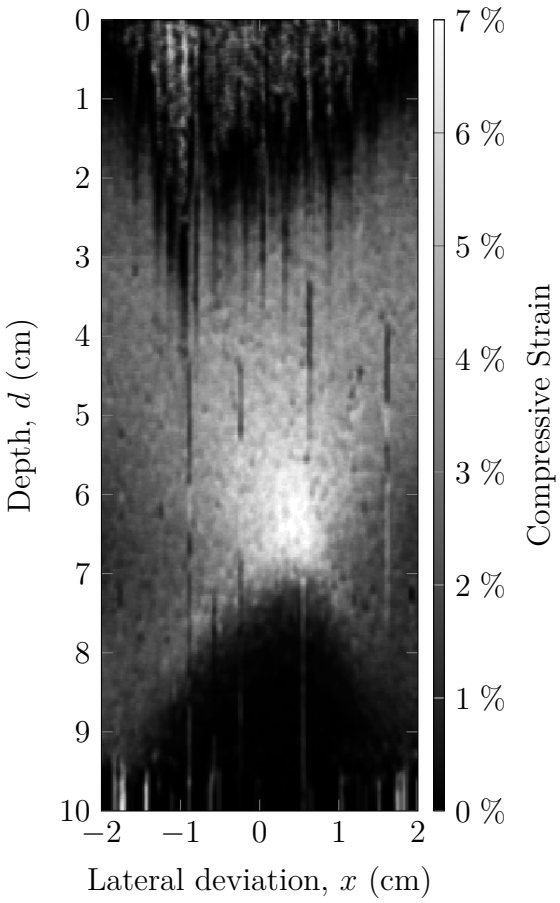

Figure 3.20: Elastogram for a 0.5 cm wide lesion embedded in the Visible Human-MRI model domain at a depth of 7.25 cm interrogated at 4 MHz with an applied strain of 2.5 %. The lesion is not visible and is the resultant elastogram.

3.3.4 Physical Phantom Validation

In order to ensure that the models presented here represented physical realities, a small subset of the cases studied were modelled in a physical phantom, specifically for three lesions with stiffness ratios of 0.56, 1.80, and 3.20 with a diameter of 2.0 cm and at a depth of 3.5 cm, interrogated at 8 MHz with approximately 5 % applied strain. The results of this study are summarized in Fig. 3.22.

As can be seen in Fig. 3.22, a relatively simple (although inexact) relationship between simulated and experimental measured strain ratios exists. It

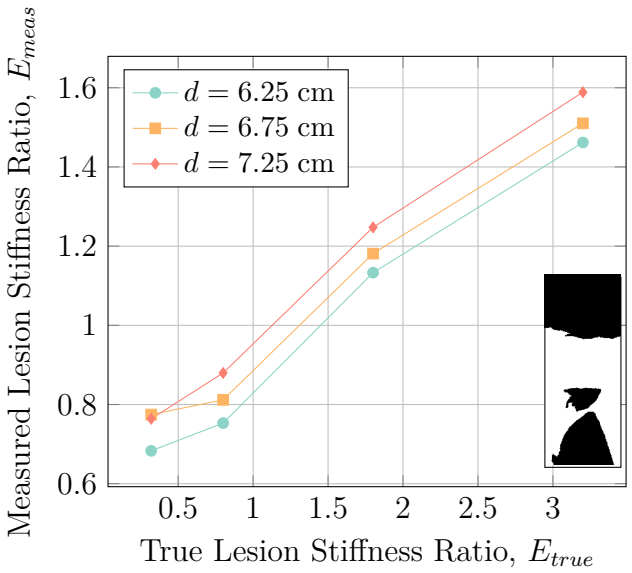

Figure 3.21: Characterization of lesion depth in a Visible Human-MRI model for lesions with a width of 2.5 cm interrogated with a 4 MHz probing frequency and 5 % applied strain. Deeper lesions (closer to the bony promience) are have slightly over-estimated lesion stiffness ratios as opposed to more superficial lesions while detection sensitivity is not affected by lesion depth.

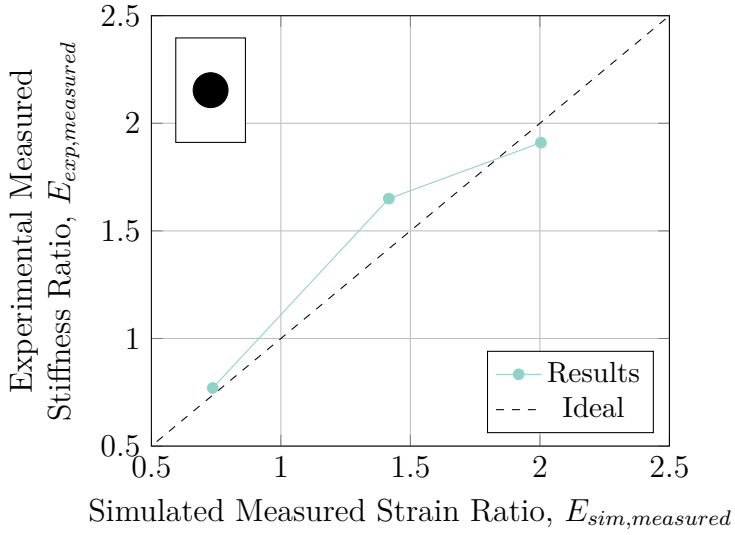

Figure 3.22: Relation between simulated measured strain ratios and experimental measured strain ratios for a lesion at a depth of 3.5 cm and diameter of 2.0 cm showing general agreement between simulated and experimental cases. Idealization errors are the most likely the cause of the differences seen between simulated and experimental cases.

must be noted that the finite-element simulations of b-mode image formation and tissue deformation presented here are idealizations of reality and idealization errors such as the ultrasound pulse profile and plane-strain assumption no doubt contributed to the difference seen in Fig. 3.22.

It must be noted that in order to acquire quasi-static elastography results in the physical phantom, the ultrasound transducer was required to be manually manipulated to cause indentation in the phantom, as the technique would most likely be performed in a clinical setting. This was found to be problematic as the ultrasound transducer was difficult to maintain perfectly perpendicular and in-plane during the compression (largely due to the necessity of using coupling ultrasonic gel). This difficulty suggests that acoustic radiation force impulse (ARFI) elastography would be a more appropriate method to acquire DTI elastograms. ARFI elastography works on the same principles as quasi-static elastography with the exception that tissue deformation is caused by localized large-amplitude acoustic waves generated by the transducer such that human factors play a far less substantial role in image acquisition.

3.4 Conclusions

With this work, we presented a numerical characterization of the use of quasi-static ultrasound elastography for the early detection of deep tissue injuries (DTI). There is a real clinical need for an objective tool that is capable of detecting the formation and progression of DTI in human subjects as these wounds are generally not visible from the surface of the skin until they have broken through and already caused substantial damage.

Through our numerical characterization, quasi-static ultrasound elastography was found to be an effective tool for detecting and monitoring DTI in

theoretical simulations. Overall, detection sensitivity was less than expected. Small lesions (with diameters $\leq$ 1.0 cm) were more difficult to differentiate due to the low lesion detection sensitivity. While lesion depth, altitude above the underlying bone, and probing frequency did not have significant effect on the lesion detection sensitivity, it was found that applying high levels of compressive strain (10 %) introduced severe error for both very soft and very stiff lesions, thus it is recommended that diagnosticians only apply moderate ($\leq$ 5 %) compressive strain when interrogating potential lesions. In the more complicated model of co-located lesions, while the separation distance between adjacent lesions did not affect the detection sensitivity, the placing of adjacent lesions generated "phantom" lesion regions with altered strain that may appear to be diseased tissue when they are in fact healthy. In a model lesion with gradual blurred boundaries, the effect of blur radius only affected the detection sensitivity and ability to differentiate soft lesions. Specifically, soft lesions with large blur radii became nearly impossible to differentiate. In the case of numerous clustered small lesions, both decreased lesion density and decreased individual lesion size caused a decrease in lesion detection sensitivity, likely due to the averaging effect of healthy tissue and diseased tissue in near proximity. Finally, in the Visible Human-MRI acquired lesion model, lesions with widths $\leq$ 1.0 cm are nearly impossible to differentiate as they are hidden by the strain field generated by the bony prominence. Lesion depth did not have an effect on the detection sensitivity, though deeper lesions (lesions which were closer to the bony prominence) had overestimated stiffnesses with respect to their more superficial counterparts.

A subset of the results found through simulation were compared with similar experiments done using a tissue mimicking phantom model. The experimental results using the phantom model generally agreed with those found

from simulation cases. It was also noted that the manual skin indentation technique involved with quasi-static ultrasound elastography proved to be difficult to produce reliable images. This difficulty suggests that an alternate method of performing ultrasound elastography may be preferable to quasi-static ultrasound elastography with manual indentation. Acoustic radiation force impulse (ARFI) elastography may be a more appropriate method to acquire DTI elastograms as although ARFI elastography works on the same principles as quasi-static elastography, the difference lays in the fact that tissue deformation is caused by localized large-amplitude acoustic waves generated by the transducer. This means that human factors play a far less substantial role in image acquisition and would likely improve repeatability and inter-operator reliability. Nevertheless, the work done here to characterize the use of quasi-static ultrasound elastography is an important step along the path of generating a useful clinical tool for detecting formative and monitoring progressive deep tissue injuries.

References

[1] T. U. S. National Library of Medicine, *Visible Human Project*, 1994.

[2] L. R. Solis, E. Twist, P. Seres, R. B. Thompson, and V. K. Mushahwar, "Prevention of deep tissue injury through muscle contractions induced by intermittent electrical stimulation after spinal cord injury in pigs.," *Journal of applied physiology (Bethesda, Md. : 1985)*, vol. 114, no. 2, pp. 286–296, Jan. 15, 2013, ISSN: 1522-1601. DOI: 10.1152/japplphysiol.00257.2012. [Online]. Available: http://dx.doi.org/10.1152/japplphysiol.00257.2012.

[3] J. C. Bamber and R. J. Dickinson, "Ultrasonic B-scanning: a computer simulation.," *Physics in medicine and biology*, vol. 25, no. 3, pp. 463–479, May 1980, ISSN: 0031-9155. [Online]. Available: http://view.ncbi.nlm.nih.gov/pubmed/7403261.

[4] T. A. Krouskop, T. M. Wheeler, F. Kallel, B. S. Garra, and T. Hall, "Elastic Moduli of Breast and Prostate Tissues under Compression," *Ultrasonic Imaging*, vol. 20, no. 4, pp. 260–274, Oct. 1, 1998, ISSN: 1096-0910. DOI: 10.1177/016173469802000403. [Online]. Available: http://dx.doi.org/10.1177/016173469802000403.

[5] A. P. Choi and Y. P. Zheng, "Estimation of Young's modulus and Poisson's ratio of soft tissue from indentation using two different-sized indentors: finite element analysis of the finite deformation effect.," *Medical & biological engineering & computing*, vol. 43, no. 2, pp. 258–264, Mar. 2005, ISSN: 0140-0118. [Online]. Available: http://view.ncbi.nlm.nih.gov/pubmed/15865137.

[6] A. D. Martin, M. Z. Daniel, D. T. Drinkwater, and J. P. Clarys, "Adipose tissue density, estimated adipose lipid fraction and whole body adiposity

in male cadavers.," *International journal of obesity and related metabolic disorders : journal of the International Association for the Study of Obesity*, vol. 18, no. 2, pp. 79–83, Feb. 1994, ISSN: 0307-0565. [Online]. Available: http://view.ncbi.nlm.nih.gov/pubmed/8148928.

[7] E. Brusseau, J. Kybic, J.-F. F. Deprez, and O. Basset, "2-D locally regularized tissue strain estimation from radio-frequency ultrasound images: theoretical developments and results on experimental data.," *IEEE transactions on medical imaging*, vol. 27, no. 2, pp. 145–160, Feb. 2008, ISSN: 0278-0062. DOI: 10.1109/tmi.2007.897408. [Online]. Available: http://dx.doi.org/10.1109/tmi.2007.897408.

Chapter 4

Numerical Characterization of Acoustic Radiation Force Impulse Imaging

4.1 Introduction

Lorem ipsum dolor sit amet, consectetuer adipiscing elit. Ut purus elit, vestibulum ut, placerat ac, adipiscing vitae, felis. Curabitur dictum gravida mauris. Nam arcu libero, nonummy eget, consectetuer id, vulputate a, magna. Donec vehicula augue eu neque. Pellentesque habitant morbi tristique senectus et netus et malesuada fames ac turpis egestas. Mauris ut leo. Cras viverra metus rhoncus sem. Nulla et lectus vestibulum urna fringilla ultrices. Phasellus eu tellus sit amet tortor gravida placerat. Integer sapien est, iaculis in, pretium quis, viverra ac, nunc. Praesent eget sem vel leo ultrices bibendum. Aenean faucibus. Morbi dolor nulla, malesuada eu, pulvinar at, mollis ac, nulla. Curabitur auctor semper nulla. Donec varius orci eget risus. Duis nibh mi, congue eu, accumsan eleifend, sagittis quis, diam. Duis eget orci sit amet orci

dignissim rutrum.

4.2 Methods

Lorem ipsum dolor sit amet, consectetuer adipiscing elit. Ut purus elit, vestibulum ut, placerat ac, adipiscing vitae, felis. Curabitur dictum gravida mauris. Nam arcu libero, nonummy eget, consectetuer id, vulputate a, magna. Donec vehicula augue eu neque. Pellentesque habitant morbi tristique senectus et netus et malesuada fames ac turpis egestas. Mauris ut leo. Cras viverra metus rhoncus sem. Nulla et lectus vestibulum urna fringilla ultrices. Phasellus eu tellus sit amet tortor gravida placerat. Integer sapien est, iaculis in, pretium quis, viverra ac, nunc. Praesent eget sem vel leo ultrices bibendum. Aenean faucibus. Morbi dolor nulla, malesuada eu, pulvinar at, mollis ac, nulla. Curabitur auctor semper nulla. Donec varius orci eget risus. Duis nibh mi, congue eu, accumsan eleifend, sagittis quis, diam. Duis eget orci sit amet orci dignissim rutrum.

4.2.1 Numerical Model

Lorem ipsum dolor sit amet, consectetuer adipiscing elit. Ut purus elit, vestibulum ut, placerat ac, adipiscing vitae, felis. Curabitur dictum gravida mauris. Nam arcu libero, nonummy eget, consectetuer id, vulputate a, magna. Donec vehicula augue eu neque. Pellentesque habitant morbi tristique senectus et netus et malesuada fames ac turpis egestas. Mauris ut leo. Cras viverra metus rhoncus sem. Nulla et lectus vestibulum urna fringilla ultrices. Phasellus eu tellus sit amet tortor gravida placerat. Integer sapien est, iaculis in, pretium quis, viverra ac, nunc. Praesent eget sem vel leo ultrices bibendum. Aenean faucibus. Morbi dolor nulla, malesuada eu, pulvinar at, mollis ac, nulla.

Curabitur auctor semper nulla. Donec varius orci eget risus. Duis nibh mi, congue eu, accumsan eleifend, sagittis quis, diam. Duis eget orci sit amet orci dignissim rutrum.

Governing Equations

The governing equations use for this model were the set of coupled first-order partial differential equations 4.1. These equations are the first-order equivalents of 4.2 taking into account acoustic absorption, tissue heterogeneities, and acoustic wave non-linearities [1].

$$\nabla^2 p - \frac{1}{c_0^2} \frac{\partial^2 p}{\partial t^2} = 0 \tag{4.2}$$

Boundary and Initial Conditions

Lorem ipsum dolor sit amet, consectetuer adipiscing elit. Ut purus elit, vestibulum ut, placerat ac, adipiscing vitae, felis. Curabitur dictum gravida mauris. Nam arcu libero, nonummy eget, consectetuer id, vulputate a, magna. Donec vehicula augue eu neque. Pellentesque habitant morbi tristique senectus et netus et malesuada fames ac turpis egestas. Mauris ut leo. Cras viverra metus rhoncus sem. Nulla et lectus vestibulum urna fringilla ultrices. Phasellus eu tellus sit amet tortor gravida placerat. Integer sapien est, iaculis in, pretium quis, viverra ac, nunc. Praesent eget sem vel leo ultrices bibendum. Aenean faucibus. Morbi dolor nulla, malesuada eu, pulvinar at, mollis ac, nulla. Curabitur auctor semper nulla. Donec varius orci eget risus. Duis nibh mi, congue eu, accumsan eleifend, sagittis quis, diam. Duis eget orci sit amet orci dignissim rutrum.

4.3 Results

Lorem ipsum dolor sit amet, consectetuer adipiscing elit. Ut purus elit, vestibulum ut, placerat ac, adipiscing vitae, felis. Curabitur dictum gravida mauris. Nam arcu libero, nonummy eget, consectetuer id, vulputate a, magna. Donec vehicula augue eu neque. Pellentesque habitant morbi tristique senectus et netus et malesuada fames ac turpis egestas. Mauris ut leo. Cras viverra metus rhoncus sem. Nulla et lectus vestibulum urna fringilla ultrices. Phasellus eu tellus sit amet tortor gravida placerat. Integer sapien est, iaculis in, pretium quis, viverra ac, nunc. Praesent eget sem vel leo ultrices bibendum. Aenean faucibus. Morbi dolor nulla, malesuada eu, pulvinar at, mollis ac, nulla. Curabitur auctor semper nulla. Donec varius orci eget risus. Duis nibh mi, congue eu, accumsan eleifend, sagittis quis, diam. Duis eget orci sit amet orci dignissim rutrum.

Chapter 5

Numerical Characterization of Shear Wave Speed Quantification

Lorem ipsum dolor sit amet, consectetuer adipiscing elit. Ut purus elit, vestibulum ut, placerat ac, adipiscing vitae, felis. Curabitur dictum gravida mauris. Nam arcu libero, nonummy eget, consectetuer id, vulputate a, magna. Donec vehicula augue eu neque. Pellentesque habitant morbi tristique senectus et netus et malesuada fames ac turpis egestas. Mauris ut leo. Cras viverra metus rhoncus sem. Nulla et lectus vestibulum urna fringilla ultrices. Phasellus eu tellus sit amet tortor gravida placerat. Integer sapien est, iaculis in, pretium quis, viverra ac, nunc. Praesent eget sem vel leo ultrices bibendum. Aenean faucibus. Morbi dolor nulla, malesuada eu, pulvinar at, mollis ac, nulla. Curabitur auctor semper nulla. Donec varius orci eget risus. Duis nibh mi, congue eu, accumsan eleifend, sagittis quis, diam. Duis eget orci sit amet orci dignissim rutrum.

Chapter 6

Conclusion

Lorem ipsum dolor sit amet, consectetuer adipiscing elit. Ut purus elit, vestibulum ut, placerat ac, adipiscing vitae, felis. Curabitur dictum gravida mauris. Nam arcu libero, nonummy eget, consectetuer id, vulputate a, magna. Donec vehicula augue eu neque. Pellentesque habitant morbi tristique senectus et netus et malesuada fames ac turpis egestas. Mauris ut leo. Cras viverra metus rhoncus sem. Nulla et lectus vestibulum urna fringilla ultrices. Phasellus eu tellus sit amet tortor gravida placerat. Integer sapien est, iaculis in, pretium quis, viverra ac, nunc. Praesent eget sem vel leo ultrices bibendum. Aenean faucibus. Morbi dolor nulla, malesuada eu, pulvinar at, mollis ac, nulla. Curabitur auctor semper nulla. Donec varius orci eget risus. Duis nibh mi, congue eu, accumsan eleifend, sagittis quis, diam. Duis eget orci sit amet orci dignissim rutrum.

6.1 Clinical Need for DTI Detection

Lorem ipsum dolor sit amet, consectetuer adipiscing elit. Ut purus elit, vestibulum ut, placerat ac, adipiscing vitae, felis. Curabitur dictum gravida mauris. Nam arcu libero, nonummy eget, consectetuer id, vulputate a, magna. Donec

vehicula augue eu neque. Pellentesque habitant morbi tristique senectus et netus et malesuada fames ac turpis egestas. Mauris ut leo. Cras viverra metus rhoncus sem. Nulla et lectus vestibulum urna fringilla ultrices. Phasellus eu tellus sit amet tortor gravida placerat. Integer sapien est, iaculis in, pretium quis, viverra ac, nunc. Praesent eget sem vel leo ultrices bibendum. Aenean faucibus. Morbi dolor nulla, malesuada eu, pulvinar at, mollis ac, nulla. Curabitur auctor semper nulla. Donec varius orci eget risus. Duis nibh mi, congue eu, accumsan eleifend, sagittis quis, diam. Duis eget orci sit amet orci dignissim rutrum.

6.2 USE Provides Potential Diagnosis Capability

Lorem ipsum dolor sit amet, consectetuer adipiscing elit. Ut purus elit, vestibulum ut, placerat ac, adipiscing vitae, felis. Curabitur dictum gravida mauris. Nam arcu libero, nonummy eget, consectetuer id, vulputate a, magna. Donec vehicula augue eu neque. Pellentesque habitant morbi tristique senectus et netus et malesuada fames ac turpis egestas. Mauris ut leo. Cras viverra metus rhoncus sem. Nulla et lectus vestibulum urna fringilla ultrices. Phasellus eu tellus sit amet tortor gravida placerat. Integer sapien est, iaculis in, pretium quis, viverra ac, nunc. Praesent eget sem vel leo ultrices bibendum. Aenean faucibus. Morbi dolor nulla, malesuada eu, pulvinar at, mollis ac, nulla. Curabitur auctor semper nulla. Donec varius orci eget risus. Duis nibh mi, congue eu, accumsan eleifend, sagittis quis, diam. Duis eget orci sit amet orci dignissim rutrum.

6.3 Future Work

Lorem ipsum dolor sit amet, consectetuer adipiscing elit. Ut purus elit, vestibulum ut, placerat ac, adipiscing vitae, felis. Curabitur dictum gravida mauris. Nam arcu libero, nonummy eget, consectetuer id, vulputate a, magna. Donec vehicula augue eu neque. Pellentesque habitant morbi tristique senectus et netus et malesuada fames ac turpis egestas. Mauris ut leo. Cras viverra metus rhoncus sem. Nulla et lectus vestibulum urna fringilla ultrices. Phasellus eu tellus sit amet tortor gravida placerat. Integer sapien est, iaculis in, pretium quis, viverra ac, nunc. Praesent eget sem vel leo ultrices bibendum. Aenean faucibus. Morbi dolor nulla, malesuada eu, pulvinar at, mollis ac, nulla. Curabitur auctor semper nulla. Donec varius orci eget risus. Duis nibh mi, congue eu, accumsan eleifend, sagittis quis, diam. Duis eget orci sit amet orci dignissim rutrum.

6.3.1 Animal Studies?

Lorem ipsum dolor sit amet, consectetuer adipiscing elit. Ut purus elit, vestibulum ut, placerat ac, adipiscing vitae, felis. Curabitur dictum gravida mauris. Nam arcu libero, nonummy eget, consectetuer id, vulputate a, magna. Donec vehicula augue eu neque. Pellentesque habitant morbi tristique senectus et netus et malesuada fames ac turpis egestas. Mauris ut leo. Cras viverra metus rhoncus sem. Nulla et lectus vestibulum urna fringilla ultrices. Phasellus eu tellus sit amet tortor gravida placerat. Integer sapien est, iaculis in, pretium quis, viverra ac, nunc. Praesent eget sem vel leo ultrices bibendum. Aenean faucibus. Morbi dolor nulla, malesuada eu, pulvinar at, mollis ac, nulla. Curabitur auctor semper nulla. Donec varius orci eget risus. Duis nibh mi, congue eu, accumsan eleifend, sagittis quis, diam. Duis eget orci sit amet orci

dignissim rutrum.

6.3.2 Human Studies?

Lorem ipsum dolor sit amet, consectetuer adipiscing elit. Ut purus elit, vestibulum ut, placerat ac, adipiscing vitae, felis. Curabitur dictum gravida mauris. Nam arcu libero, nonummy eget, consectetuer id, vulputate a, magna. Donec vehicula augue eu neque. Pellentesque habitant morbi tristique senectus et netus et malesuada fames ac turpis egestas. Mauris ut leo. Cras viverra metus rhoncus sem. Nulla et lectus vestibulum urna fringilla ultrices. Phasellus eu tellus sit amet tortor gravida placerat. Integer sapien est, iaculis in, pretium quis, viverra ac, nunc. Praesent eget sem vel leo ultrices bibendum. Aenean faucibus. Morbi dolor nulla, malesuada eu, pulvinar at, mollis ac, nulla. Curabitur auctor semper nulla. Donec varius orci eget risus. Duis nibh mi, congue eu, accumsan eleifend, sagittis quis, diam. Duis eget orci sit amet orci dignissim rutrum.

Appendix A

Data Tables

Lorem ipsum dolor sit amet, consectetuer adipiscing elit. Ut purus elit, vestibulum ut, placerat ac, adipiscing vitae, felis. Curabitur dictum gravida mauris. Nam arcu libero, nonummy eget, consectetuer id, vulputate a, magna. Donec vehicula augue eu neque. Pellentesque habitant morbi tristique senectus et netus et malesuada fames ac turpis egestas. Mauris ut leo. Cras viverra metus rhoncus sem. Nulla et lectus vestibulum urna fringilla ultrices. Phasellus eu tellus sit amet tortor gravida placerat. Integer sapien est, iaculis in, pretium quis, viverra ac, nunc. Praesent eget sem vel leo ultrices bibendum. Aenean faucibus. Morbi dolor nulla, malesuada eu, pulvinar at, mollis ac, nulla. Curabitur auctor semper nulla. Donec varius orci eget risus. Duis nibh mi, congue eu, accumsan eleifend, sagittis quis, diam. Duis eget orci sit amet orci dignissim rutrum.

A.1 Quasi-Static Ultrasound Elastography

Lorem ipsum dolor sit amet, consectetuer adipiscing elit. Ut purus elit, vestibulum ut, placerat ac, adipiscing vitae, felis. Curabitur dictum gravida mauris. Nam arcu libero, nonummy eget, consectetuer id, vulputate a, magna. Donec

vehicula augue eu neque. Pellentesque habitant morbi tristique senectus et netus et malesuada fames ac turpis egestas. Mauris ut leo. Cras viverra metus rhoncus sem. Nulla et lectus vestibulum urna fringilla ultrices. Phasellus eu tellus sit amet tortor gravida placerat. Integer sapien est, iaculis in, pretium quis, viverra ac, nunc. Praesent eget sem vel leo ultrices bibendum. Aenean faucibus. Morbi dolor nulla, malesuada eu, pulvinar at, mollis ac, nulla. Curabitur auctor semper nulla. Donec varius orci eget risus. Duis nibh mi, congue eu, accumsan eleifend, sagittis quis, diam. Duis eget orci sit amet orci dignissim rutrum.

A.2 Acoustic Radiation Force Impulse Imaging

Lorem ipsum dolor sit amet, consectetuer adipiscing elit. Ut purus elit, vestibulum ut, placerat ac, adipiscing vitae, felis. Curabitur dictum gravida mauris. Nam arcu libero, nonummy eget, consectetuer id, vulputate a, magna. Donec vehicula augue eu neque. Pellentesque habitant morbi tristique senectus et netus et malesuada fames ac turpis egestas. Mauris ut leo. Cras viverra metus rhoncus sem. Nulla et lectus vestibulum urna fringilla ultrices. Phasellus eu tellus sit amet tortor gravida placerat. Integer sapien est, iaculis in, pretium quis, viverra ac, nunc. Praesent eget sem vel leo ultrices bibendum. Aenean faucibus. Morbi dolor nulla, malesuada eu, pulvinar at, mollis ac, nulla. Curabitur auctor semper nulla. Donec varius orci eget risus. Duis nibh mi, congue eu, accumsan eleifend, sagittis quis, diam. Duis eget orci sit amet orci dignissim rutrum.

A.3 Shear Wave Speed Quantification

Lorem ipsum dolor sit amet, consectetuer adipiscing elit. Ut purus elit, vestibulum ut, placerat ac, adipiscing vitae, felis. Curabitur dictum gravida mauris. Nam arcu libero, nonummy eget, consectetuer id, vulputate a, magna. Donec vehicula augue eu neque. Pellentesque habitant morbi tristique senectus et netus et malesuada fames ac turpis egestas. Mauris ut leo. Cras viverra metus rhoncus sem. Nulla et lectus vestibulum urna fringilla ultrices. Phasellus eu tellus sit amet tortor gravida placerat. Integer sapien est, iaculis in, pretium quis, viverra ac, nunc. Praesent eget sem vel leo ultrices bibendum. Aenean faucibus. Morbi dolor nulla, malesuada eu, pulvinar at, mollis ac, nulla. Curabitur auctor semper nulla. Donec varius orci eget risus. Duis nibh mi, congue eu, accumsan eleifend, sagittis quis, diam. Duis eget orci sit amet orci dignissim rutrum.

Appendix B

Source Code

Lorem ipsum dolor sit amet, consectetuer adipiscing elit. Ut purus elit, vestibulum ut, placerat ac, adipiscing vitae, felis. Curabitur dictum gravida mauris. Nam arcu libero, nonummy eget, consectetuer id, vulputate a, magna. Donec vehicula augue eu neque. Pellentesque habitant morbi tristique senectus et netus et malesuada fames ac turpis egestas. Mauris ut leo. Cras viverra metus rhoncus sem. Nulla et lectus vestibulum urna fringilla ultrices. Phasellus eu tellus sit amet tortor gravida placerat. Integer sapien est, iaculis in, pretium quis, viverra ac, nunc. Praesent eget sem vel leo ultrices bibendum. Aenean faucibus. Morbi dolor nulla, malesuada eu, pulvinar at, mollis ac, nulla. Curabitur auctor semper nulla. Donec varius orci eget risus. Duis nibh mi, congue eu, accumsan eleifend, sagittis quis, diam. Duis eget orci sit amet orci dignissim rutrum.

B.1 Quasi2DUltrasound

Lorem ipsum dolor sit amet, consectetuer adipiscing elit. Ut purus elit, vestibulum ut, placerat ac, adipiscing vitae, felis. Curabitur dictum gravida mauris. Nam arcu libero, nonummy eget, consectetuer id, vulputate a, magna. Donec

vehicula augue eu neque. Pellentesque habitant morbi tristique senectus et netus et malesuada fames ac turpis egestas. Mauris ut leo. Cras viverra metus rhoncus sem. Nulla et lectus vestibulum urna fringilla ultrices. Phasellus eu tellus sit amet tortor gravida placerat. Integer sapien est, iaculis in, pretium quis, viverra ac, nunc. Praesent eget sem vel leo ultrices bibendum. Aenean faucibus. Morbi dolor nulla, malesuada eu, pulvinar at, mollis ac, nulla. Curabitur auctor semper nulla. Donec varius orci eget risus. Duis nibh mi, congue eu, accumsan eleifend, sagittis quis, diam. Duis eget orci sit amet orci dignissim rutrum.